bioRχiv Submission Template bioRχiv Submission Template bioRχiv Submission Template bioRχiv Submission Template bioRχiv Submission Template bioRχiv Submission Template bioRχiv Submission Template

RESEARCH ARTICLE

The complex genetics of symbiotic extended phenotypes across environments in a model mutualism

Rebecca T. Batstone,[a,*] Hanna Lindgren,[b] Cassandra M. Allsup,[b] Laura A. Goralka,[b] Alex B. Riley,[b] Michael A. Grillo,[c] Amy Marshall-Colon,[a,b] Katy D. Heath,[a,b,*]

Carl R. Woese Institute for Genomic Biology, University of Illinois at Urbana-Champaign, 1206 West Gregory Drive, Urbana, IL 61801 USA[a]; Department of Plant Biology, University of Illinois at Urbana-Champaign, 286 Morrill Hall, 505 South Goodwin Avenue, Urbana, IL 61801 USA[b]; Department of Biology, Loyola University Chicago, 1032 W. Sheridan Road, Chicago, IL 60618 USA[c]

R. Batstone and H. Lindgren contributed equally. Author order was determined based on overall contribution, particularly time spent analyzing the data, as well as writing and compiling feedback.

Compiled October 1, 2021
This is a draft manuscript, pre-submission

* Co-corresponding authors:
R. Batstone, rtbatstone@gmail.com
K. Heath, kheath@iliinois.edu.

Authorship statement: KDH and AMC conceived of the work, acquired funding, and designed the experiments. MAG collected soil, performed trapping experiments, and isolated strains. ABR performed preliminary experiments and extracted DNA. HL and CMA led experimental work and data collection with assistance from LAG, ABR, KDH, RTB, and AMC. RTB, HL, and KDH performed data analysis and interpretation. KDH, RTB, and HL drafted the article. All authors participated in critical revisions and approved the final version for submission.

ABSTRACT A goal of modern biology is to develop the genotype-phenotype (G→P) map, a predictive understanding of how genomic information generates trait variation that forms the basis of both natural and managed communities. As microbiome research advances, however, it has become clear that many of these traits are symbiotic extended phenotypes, being governed by genetic variation encoded not only by the host's own genome, but also by the genomes of myriad cryptic symbionts. Building a reliable G→P map therefore requires accounting for the multitude of interacting genes and even genomes involved in symbiosis. Here we use naturally-occurring genetic variation in 191 strains of the model nitrogen-fixing symbiont *Ensifer meliloti* in four mapping experiments to study the genomic architecture of a key symbiotic extended phenotype - partner quality, or the fitness benefit conferred to a host by a particular symbiont genotype, within and across environmental contexts and host genotypes. We define three novel categories of loci in rhizobium genomes that must be accounted for if we want to build a reliable G→P map of partner quality; namely, 1) loci whose function in partner quality depends on the environment, 2) those that depend on the host genotype with which rhizobia interact, and 3) universal loci that are likely important in all or most environments.

IMPORTANCE Given the rapid rise of research on how microbiomes can be harnessed to improve host health, understanding the contribution of microbial genetic variation to host phenotypic variation is pressing, and will better enable us to predict the evolution of (and select more precisely for) symbiotic extended phenotypes that impact host health. We uncover extensive context-dependency in both the identity and functions of symbiont loci that control host growth, which will make it harder to predict the genes and pathways important for determining symbiotic outcomes under different conditions. Despite this context-dependency, we also resolve a core set of universal loci that are likely important in all or most environments, and thus, serve as excellent targets both for genetic engineering and future coevolutionary studies of symbiosis.

KEYWORDS: GWAS, mapping, *Medicago truncatula*, *Ensifer meliloti*, symbiosis, partner quality, rhizobium, GxE, GxG, genotype-phenotype map, G→P map, root nodule, nodulation, symbiotic nitrogen fixation

bioRχiv Submission Template bioRχiv Submission Template bioRχiv Submission Template bioRχiv Submission Template bioRχiv Submission Template bioRχiv Submission Template bioRχiv Submission Template

INTRODUCTION

We live in a symbiotic world. It is increasingly recognized that many important traits, including human metabolism, insect diet and defense, and plant nutrient foraging, are actually *symbiotic extended phenotypes* governed (at least in part) by cryptic variation in their microbial symbionts (e.g., 1, 2, 3, 4, 5, 6, 7; reviewed by 8, 9, 10, 11, 12). Incorporating the complex genetics arising from these interactions, however, has lagged behind understanding their ecological outcomes. Characterizing the genetic basis of these cross-domain relationships represents a symbiotic extension of the genotype-phenotype (G→P) map (13, 14, 15), wherein genetic variation present in symbionts (G) presents as phenotypic variation (P) expressed by the host. In symbiosis, as in all organisms, the G→P map is a crucial step towards a predictive understanding of evolution (e.g., a trait's genomic architecture influences the rates and trajectories of its response to selection), and for bioengineering, where we must know not only which genes to target and exactly how to edit them, but also anticipate how consistent the knock-on effects will be across diverse environments and/or genetic backgrounds (16, 17).

A key lesson from studies of the G→P map within single organisms is that phenotypic variation fundamentally arises in non-additive ways as genomic variation is filtered through "layer(s) of context-dependence" (14) including genotype-by-environment interactions, epistasis, and pleiotropy (18, 19, 20, 21, 15, 22, 23). The role of context-dependency in the G→P is particularly relevant for symbiotic extended phenotypes, given the potential for higher-order interactive genetic effects. For example, interacting genomes can generate genotype-by-genotype interactions between host and symbiont (intergenomic epistasis, or G × G: 24, 25, 26, 27, 28, 29) and even G × G × E whereby trait values depend not only on the interaction of alleles in both partners, but on the environmental context (30, 31, 32). Such complex context-dependent effects are critical for evolution; for example, G × G × E for fitness is the statistical expression of the coevolutionary selection mosaic (33, 34, 27). Additionally, genes that consistently affect symbiotic extended phenotypes arising in plant-microbe interactions, independent of these layers of context dependency, are important targets for breeding and bioengineering (9, 35, 16, 36, 37). Fine-scale mapping of the loci contributing to symbiotic extended phenotypes across partner genotype and environmental contexts can therefore generate a more holistic picture of both types of genetic effects (i.e., the genes that universally contribute and those that are context-dependent), and thus, provides insights both for natural (co)evolutionary processes and sustainable agriculture.

The symbiosis between nitrogen-fixing rhizobia and leguminous plants has been a key model for addressing both additive and interactive genetic effects in symbiosis (i.e., G × G, G × E: 38, 39, 40, 41, 42), with resequencing projects, germplasm collections, and many genetic and genomic tools, particularly in *Medicago-Ensifer* interactions (43, 44, 45, 46, 47). These symbioses are also major drivers of the terrestrial nitrogen (N) cycle, contributing up to 21 million tonnes of fixed N each year (48, 49). In their specialized root nodules, legumes trade photosynthetically-derived fixed carbon in exchange for N fixed by the rhizobia, making legumes keystone members of natural plant communities and important staples of sustainable agriculture (reviewed by 50, 51). Rhizobial genomes themselves have been studied as models of bacterial genome evolution, reflecting the dynamic tension between the core set of genes, often on the main chromosome, and the more flexible genes, often found on mobile plasmids, islands, and other elements (52, 53, 54, 55, 56). Symbiosis plasmids in particular often show abundant recombination (45, 57, 58), allowing genome-wide association

bioRχiv Submission Template bioRχiv Submission Template bioRχiv Submission Template bioRχiv Submission Template bioRχiv Submission Template bioRχiv Submission Template bioRχiv Submission Template

studies (GWAS) to detect associations between individual genomic variants and traits of interest (59, 45, 60, 61, 56). This symbiosis is thus well poised for understanding the genetic basis of important symbiotic extended phenotypes.

Decades of functional genetic studies have resolved a number of symbiosis genes, mostly those that disrupt symbiosis when knocked out (reviewed by 62, 63), enabling increasingly well-resolved models for how interactions establish and how trade is coordinated (64). Nevertheless, mapping efforts in legume-rhizobium symbiosis, which leverage standing genetic variation, indicate that a much broader set of genes and genetic pathways contribute to the quantitative variation in partner quality that we know to be important in natural and managed systems (46, 59, 45, 65, 66). Thus quantitative genetic mapping efforts can generate novel candidate genes for symbiosis while shedding light on the G→P map of symbiotic extended phenotypes in nature.

Here we study the complex genetic basis and layers of context-dependency in the G→P map of an ecologically-important symbiotic extended phenotype: partner quality, or the fitness benefit a legume host receives when in association with a particular rhizobium strain, which not only impacts plant fitness, but also the nutritional composition of leaves, as high-quality rhizobia fix more atmospheric N that plants can incorporate into their tissues. Using a panel of 191 strains of the model rhizobium *Ensifer meliloti* isolated from natural populations in the native range, we 1) ask whether the genetic architecture of rhizobium partner quality differs across environments and across host genotypes, or alternatively if variation at a core set of rhizobium genes control partner quality in all contexts; 2) study how the three genomic elements of *E. meliloti* contribute to partner quality variation across two host genotypes and in multiple environments, validating the functional division of labour of these elements in nature; and finally, 3) suggest candidate metabolic functions and genetic loci that are responsible for both context-dependency as well as universally-beneficial effects that are consistent across environments.

RESULTS

Our phenotypic and genetic analyses suggest important roles for context-dependency in the genetic control of symbiotic extended phenotypes. Overall, we found 1,453 variants (**Supp. Dataset S1**) in 746 (**Supp. Dataset S2**) unique coding genes associated with shoot biomass, our focal rhizobium partner quality phenotype, while 5,402 variants (**Supp. Dataset S3**) and 1,770 coding genes (**Supp. Dataset S4**) were associated with at least one partner quality phenotype analyzed in this study (i.e., shoot biomass, chlorophyll A, plant height, leaf number); an additional 572 variants fell into 369 distinct non-coding regions (**Supp. Dataset S3**).

Three categories of G→P associations emerged from our analyses (**Fig. 1**; see **Supp. Fig. S1** for other traits). First were conditional associations that depended on the environment (G × E: comparing experiments within host lines, **Fig. 1A**); 510 (68%) were found in only one of the four experiments. Second were "G × G genes", the 51 (7%) genes that were associated with partner quality in both experiments with one host genotype but were found in neither experiment with the other host genotype (**Fig. 1A**). Specifically, 18 A17-specific genes were found in both experiments with this host (but never with DZA), while 33 DZA-specific genes were found in both experiments with this host (but never with A17). Last, but not least, were "universal" genes, the 60 (8%) genes that were found to be associated with rhizobium partner quality independent of host genotype or environment (union in the center of **Fig. 1A**). Specifically, while only five of these genes were associated with partner quality in all four experiments, 55 additional genes were found in three of the four experiments and thus are strong

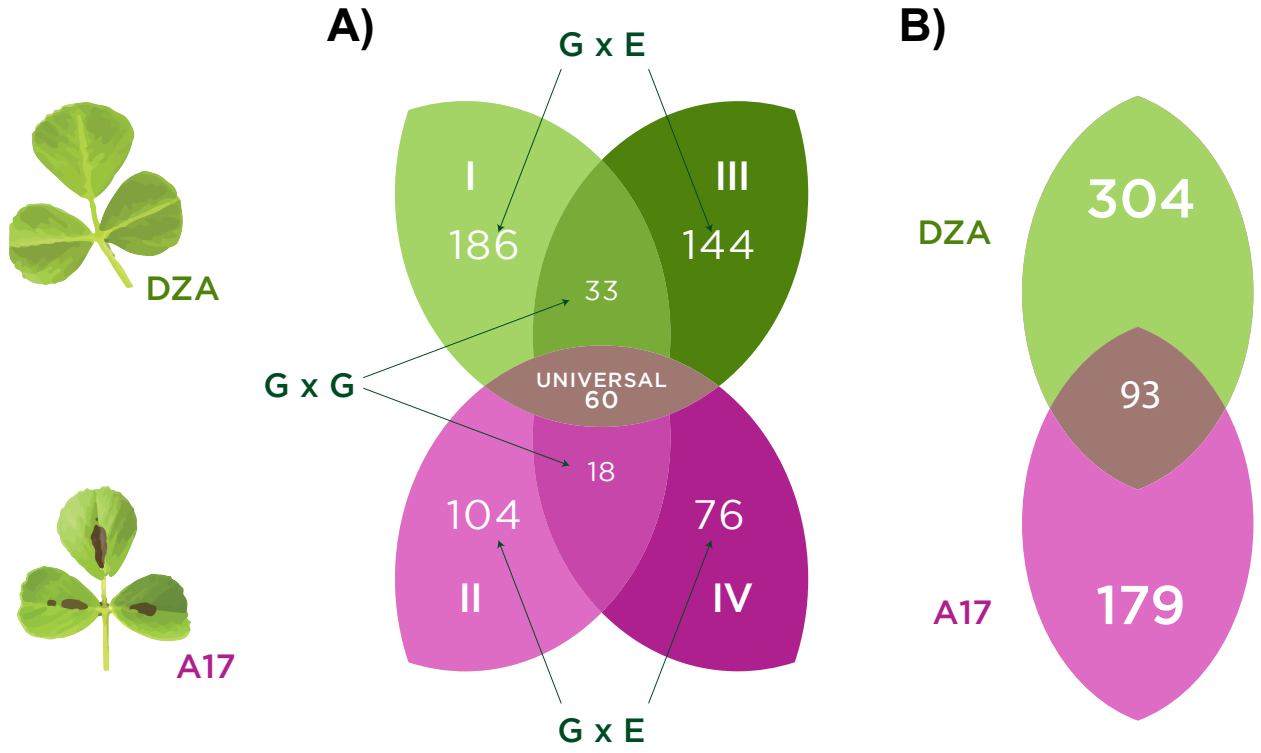

FIG 1 Association mapping of partner quality reveals strong signatures of environmental-dependence. Venn diagram showing number of rhizobium (*E. meliloti*) genes significantly associated with plant (*M. truncatula*) aboveground biomass (one metric of symbiotic partner quality) in A) each of four separate mapping experiments with either host line DZA (I and III in green) or host line A17 (II and IV in pink). Green and pink unions represent genes contributing to plant biomass in both experiments with either DZA or A17, respectively, while the mauve oval in the center represents universal genes found to contribute to plant aboveground biomass in at least three of the four experiments. B) Genes significantly associated with cross-experiment plasticity in plant aboveground biomass for host genotype DZA in green (experiments I vs. III), A17 in pink (experiments II vs. IV), or independently associated with plasticity in both hosts (central mauve triangle).

candidates for contributing to partner quality in many conditions. We discuss these three types of genetic effects in turn, at the phenotypic, genomic (three elements in the tripartite genome), gene, and variant level, then conclude with the general implications of our findings for plant-microbe interactions and symbiosis evolution more broadly.

Genotype-by-environment interactions in the G→P map of symbiotic partner quality. Environmental dependence was a pervasive pattern at both the phenotypic, genomic, and individual gene levels, suggesting that different sets of rhizobium genes contribute to symbiotic partner quality under different environmental conditions. At the phenotypic level, ANOVA indicated abundant genetic variance in partner quality traits, including both significant main effects of strain as well as strong strain-by-experiment (G × E) interactions (see **Table 1** and within-experiment heritabilities in **Table 2**). Cross-environment genetic correlations (r) of strain means between experiments within a host line were generally significant (**Table 2**), consistent with strain main effects (some strains had consistently higher partner quality than others; see **Supp. Figs. S2** and **S3** for all within and between experiment trait correlations). Nev-

bioRχiv Submission Template bioRχiv Submission Template bioRχiv Submission Template bioRχiv Submission Template bioRχiv Submission Template bioRχiv Submission Template bioRχiv Submission Template

bioRχiv Submission Template bioRχiv Submission Template bioRχiv Submission Template bioRχiv Submission Template bioRχiv Submission Template bioRχiv Submission Template bioRχiv Submission Template

TABLE 1 Linear mixed model genotype by environment (G x E) ANOVAs for square-root transformed traits measured on plant lines A17 (left) and DZA (right). Numbers outside of and within parantheses in columns "A17" and "DZA" represent χ^2 values and degrees of freedom. Rack included as a random effect, while all other terms are fixed. Significance of rack determined by calculating the log likelihood ratio between models with and without the random effect of rack.

Trait	Model term	A17	DZA
Chlorophyll	Intercept	619.4(1)***	1447.65(1)***
	Strain	252.6(190)**	361.67(190)***
	Experiment	0.15(1)	0(1)
	Strain X Experiment	191.38(182)	205.16(183)
	Rack	30.86(1)***	23.91(1)***
Plant height	Intercept	373.58(1)***	355.55(1)***
	Strain	340.68(190)***	268.05(190)***
	Experiment	20.24(1)***	2.5(1)
	Strain X Experiment	308.63(185)***	177.71(183)
	Rack	38.35(1)***	54.12(1)***
Leaves	Intercept	207.69(1)***	164.09(1)***
	Strain	355.37(190)***	207.58(190)
	Experiment	7.85(1)**	0.45(1)
	Strain X Experiment	243.88(185)**	218.54(183)*
	Rack	27.51(1)***	41.67(1)***
Shoot biomass	Intercept	97.65(1)***	179.32(1)***
	Strain	544.81(190)***	499.67(190)***
	Experiment	10.08(1)**	6.93(1)**
	Strain X Experiment	330.06(185)***	262.2(183)***
	Rack	11.32(1)***	155.67(1)***

Significance: $p < 0.001$ = '***'; $p < 0.01$ = '**'; $p < 0.05$ = '*'

TABLE 2 Within-experiment broad-sense heritabilities (H^2) and cross-environment genetic correlations (*r*). G × E interactions were partitioned into changes in variance versus rank order (i.e., crossing), and the percent due to crossing is presented. Experiments (exps.) 1 and 3 for DZA, 2 and 4 for A17.

Trait	Plant line	H^2 (exps. 1/2)	H^2 (exps. 3/4)	*r*	Crossing (%)
Shoot biomass	A17	0.302***	0.262***	0.221**	99.83
Chlorophyll		0	0.093*	0.201**	0
Plant height		0.181***	0.173***	0.1	73.37
Leaves		0.173***	0.127***	0.173*	94.13
Shoot biomass	DZA	0.248***	0.253***	0.265***	87.19
Chlorophyll		0.118*	0.141***	0.297***	99.06
Plant height		0.131**	0.065*	0.175*	99.97
Leaves		0.05	0.084*	-0.071	63.97

Significance: $p < 0.001$ = '***'; $p < 0.01$ = '**'; $p < 0.05$ = '*'

ertheless, for most traits in both hosts, G × E was driven by changes in the rank order of strain means across environments (**Table 2** crossing (%); see **Supp. Fig. S4** for reaction norms). Rhizobium strains varied considerably in cross-environment plasticity for shoot biomass, with some strains having consistently low/high partner quality (i.e., resulting in small/large plant biomass, respectively) independent of the environment, while others responded strongly to the environmental differences between experiments (**Supp. Fig. S5**).

At the genomic-level, our evidence indicates that G × E was driven by small-scale shifts in the identity, and estimated allelic effects, of individual loci across environments rather than large shifts in which genomic elements have contributed to partner quality variation (**Supp. Fig. S6**). The vast majority of genes contributing to partner quality variation were located on the symbiotic elements (megaplasmid pSymA or chromid pSymB; **Fig. 2**; **Supp. Dataset S2**; see **Supp. Fig. S7** for other traits), although some environmentally-dependent loci were found on the chromosome (i.e., G × E and plasticity). Within host lines, 330 total genes were mapped with host line DZA (186 and 144 in experiments 1 and 3, respectively), while only 180 total genes mapped to host line A17 (104 and 76 in experiments 2 and 4, respectively; **Fig. 1A**).

At the gene-level, for experiment 1 in host line DZA, the INTERPRO terms "Transcription regulator *hth*, *lac*I" and "Lambda repressor-like, DNA-binding domain" were marginally significantly enriched (p = 0.00101 and 0.00482, respectively), as was the "Oxidative phosphorylation" KEGG pathway (p = 0.00959; **Supp. Dataset S5**), whereas for experiment 3 in host line DZA, the "Benzoate degradation" KEGG pathway was significantly enriched (FDR-corrected p = 0.00880), while the GO terms "3,4-dihydroxybenzoate catabolic process" and "transmembrane transport" were marginally significantly enriched (p = 0.00204 and 0.00376, respectively; **Supp. Dataset S5**). For experiment 2 in host line A17, the GO terms "transcription, DNA-templated" were significantly enriched (FDR corrected p = 0.00143), as were the related UNIPROT keywords for "transcription regulation" (FDR corrected p = 0.00310) and "DNA-binding" (p = 0.00310; **Supp. Dataset S5**), whereas for experiment 4 in host line A17, the INTERPRO term "Amidohydrolase 1" was marginally significantly enriched (p = 0.0307; **Supp. Dataset S5**). Overall, many of the underlying molecular processes important for driving variation in partner quality appear to be environmentally-dependent, making it harder to predict which genes and pathways will be important for determining symbiotic outcomes under different conditions.

At the variant-level, for each host (DZA or A17), we used correlations of the es-

bioRχiv Submission Template

bioRχiv Submission Template bioRχiv Submission Template bioRχiv Submission Template bioRχiv Submission Template bioRχiv Submission Template bioRχiv Submission Template bioRχiv Submission Template

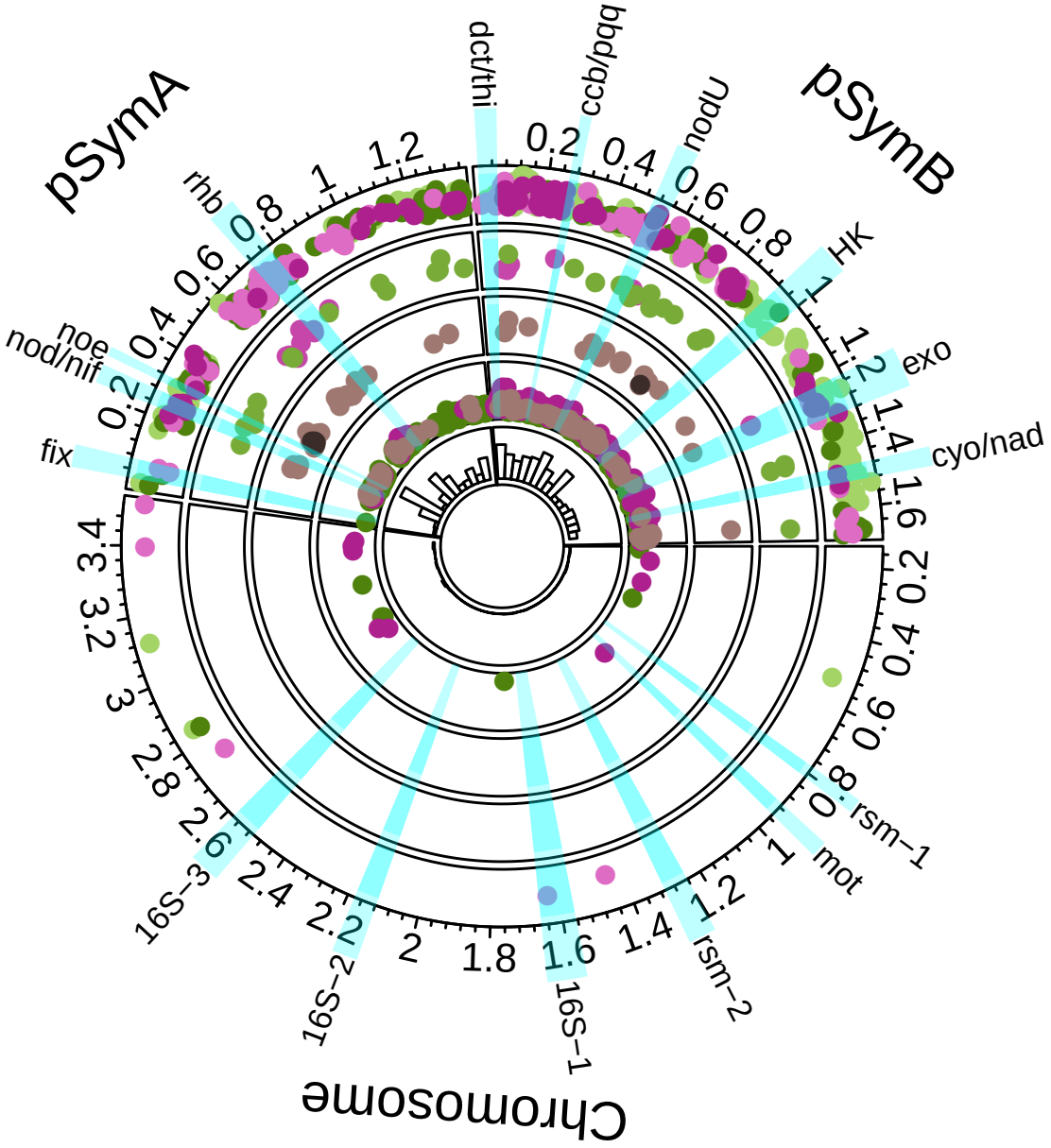

FIG 2 **Loci associated with partner quality are mostly limited to the symbiosis plasmids. Circos plot showing positions of genes (dots) significantly associated with shoot biomass. Each ring represents a different gene category, outermost to innermost: 1) G x E, 2) G x G, 3) partially universal and universal, 4) plasticity, while 5) depicts a histogram based on the total number of significant genes across 100 kbp-sized windows. The x- and y-axes for rings 1-4 represent genomic position (Mbp) and average absolute effect sizes of variants within each gene, respectively. The colours reflect categories in the Venn Diagrams: for rings 1, 2, and 4, genes associated with DZA-only traits are represented by shades of green, on A17-only with shades of purple, and both hosts in mauve (ring 4). For ring 3, genes associated with both hosts in more than three environments are represented in mauve (i.e., "partially universal"), and universal genes in black. Relevant loci are highlighted in blue, with abbreviations for clusters on the outer circle as specified in Supp. Fig. S7.**

bioRχiv Submission Template bioRχiv Submission Template bioRχiv Submission Template bioRχiv Submission Template bioRχiv Submission Template bioRχiv Submission Template bioRχiv Submission Template

timated allelic effects to assess the degree to which the individual effects of rhizobium alleles on partner quality were consistent in direction and/or magnitude, or whether they depended on the environment. When variants were significantly associated with partner quality in both experiments, they tended to have inconsistent effects for host line DZA, while being more consistent for A17 (dotted coloured lines in **Fig. 3A,B**, respectively). In fact, on A17, all of the nearly-universal variants (**Fig. 3B** black dots) had concordant (i.e., same-sign) effects on shoot biomass between experiments, whereas the opposite was true for DZA (**Fig. 3A** black dots) - all nearly-universal variants had discordant (i.e., opposite-sign) effects between experiments. For host line DZA, 12 particularly interesting variants had significant but opposing effects on plant biomass across the two experiments (**Fig. 3A**). Such associations might point to interesting environmentally-dependent genes, including the glycan metabolism gene *kdul*l1 (SMa0214/NP_435359.2), and the ornithine decarboxylase gene *spe*C (Smed_5195/YP_001313905.1; **Supp. Dataset S1**). Regardless of host line, however, the vast majority of variants in our studies had conditionally-neutral effects, even those with large magnitude (**Fig. 3**; **Supp. Fig. S8** for other traits), and for both hosts, we rejected the global null hypothesis that allelic effects were the same across experiments (both $p < 0.0001$; **Supp. Fig. S9**).

Next we mapped the among-strain differences in plasticity (**Supp. Fig. S5**) to identify specific loci contributing to G × E. At the genomic-level, most (63%) plasticity loci were found on pSymB (**Fig. 2**; **Supp. Fig. S6B**). Of 576 genes, 400 (69%) were also associated with shoot biomass variation *within* at least one of the four experiments when each was mapped independently, indicating abundant overlap in the genetic architecture of both within- and among-environment partner quality variation (**Supp. Dataset S6**). Plasticity loci were marginally significantly enriched for the INTERPRO terms "Ti-type conjugative transfer relaxase *tra*A" ($p = 0.0292$) and "*mob*A/*mob*L protein" ($p = 0.0292$), as well as several INTROPRO terms containing "tetratricopeptide-repeat" (p range: 0.006 to 0.0310), among others (**Supp. Dataset S5**). Of 576 total plasticity genes, only 93 (16%) were mapped in both host genotypes (**Fig. 1B**, **Fig. 2**; **Supp. Dataset S7**). Perhaps most interesting are the 14 of these plasticity genes that were *not* associated with variation within any of the four experiments when mapped separately (**Supp. Dataset S6**); these loci are particularly strong candidates for understanding how G x E in rhizobia scales up to alter host growth, and none to our knowledge have known functional roles in symbiosis.

The genetic architecture of rhizobium partner quality depends on host genotype. Given our four-experiment design, we used the conservative approach of only considering G × G genes to be those that were associated with partner quality in *both* experiments with one host genotype and *neither* of the other. We found 33 genes that contributed to partner quality but only in DZA, and 18 that contributed but only in A17 (**Fig. 1**; **Supp. Dataset S2**). These genes split evenly across the two symbiosis plasmids of the genome (pSymA: N = 24; pSymB: N = 27). Below, we discuss our results at the gene-level for each host separately.

In the list of A17-only G x G genes, analyses of UNIPROT keywords indicated that "Selenium" was marginally significantly overrepresented ($p = 0.00771$), while GO terms for "transferase activity, transferring glycosyl groups" were marginally overrepresented ($p = 0.0417$; **Supp. Dataset S5**). Notably, these genes include both *exo*U (SMb20948/NP_437611.1) and *exo*W (SMb21690/NP_437613.1; **Supp. Dataset S2**), two glucosyltransferases critical for adding the 6th and 7th sugars (respectively) on the succinoglycan molecule, an exopolysaccharide required for infection thread formation and thus host plant invasion for effective symbiosis (67, 68, 69). Non-functional *exo* genes

bioRχiv Submission Template bioRχiv Submission Template bioRχiv Submission Template bioRχiv Submission Template bioRχiv Submission Template bioRχiv Submission Template bioRχiv Submission Template bioRχiv Submission Template

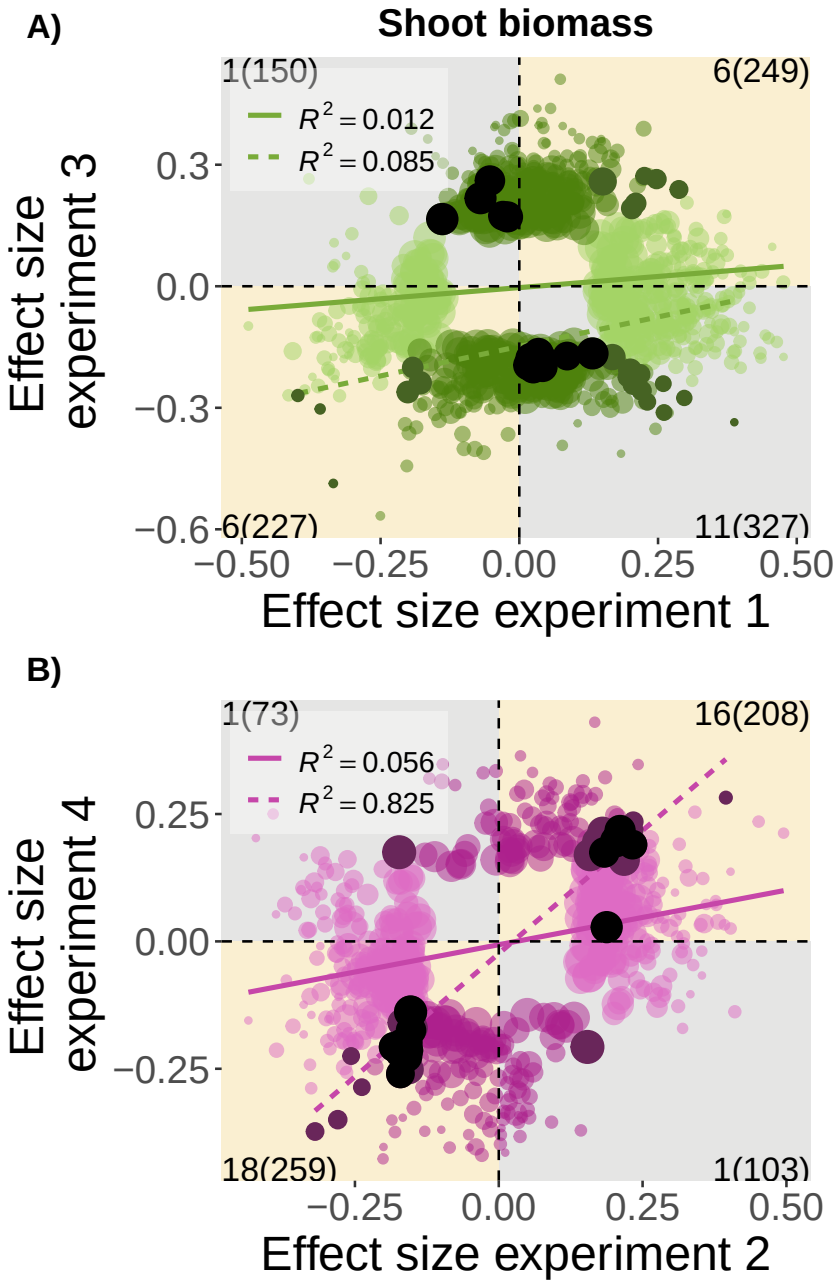

FIG 3 **Allelic effects are more consistent between experiments for A17, but not for DZA. Correlations between the estimated allelic effects of individual *E. meliloti* variants on plant shoot biomass (from GWAS) in each of two experiments for either A) host DZA (green) or B) A17 (pink). Only allelic effects that were significant in one (lighter colours) or both (dark points) environments are shown, while black dots represent nearly universal variants, i.e., associated with the same trait in three experiments. Linear relationships and R^2 values are depicted for all variants (solid coloured line) or variants significant in both experiments (dotted coloured line). Counts of significant variants for one or both environments appear in the corners of each quadrant within or outside the parentheses, respectively.**

bioRχiv Submission Template bioRχiv Submission Template bioRχiv Submission Template bioRχiv Submission Template bioRχiv Submission Template bioRχiv Submission Template bioRχiv Submission Template

are known to result in less-efficient, though sometimes not entirely deficient, symbiosis (70). Together with this prior knowledge, our finding that variants in two succinoglycan biosynthesis enzymes affected host biomass production in host A17 suggests a strong role for succinoglycan-mediated host invasion in mediating symbiotic benefits in natural populations. Future studies of coevolution between succinoglycan structure and host plant detection would likely be fruitful. Also notable is *sel*A (SMa0011/NP_435251.1; **Supp. Dataset S2**), a transferase required for the biosynthesis of selenocysteine, a less-used amino acid incorporated into select proteins in only about 20% of bacterial genomes (71, 72, 73). To our knowledge, nothing is known about the role of selenocysteine in rhizobia or in legume-rhizobium symbiosis.

By contrast, the list of DZA-only G × G genes was dominated by GO terms "transcription factor activity, sequence-specific DNA binding" ($p = 0.0247$) and "cellular amino acid metabolic process" ($p = 0.0425$; **Supp. Dataset S5**). Notably this list contains three *lys*R transcriptional regulators (**Supp. Dataset S2**) of at least 90 in the genome: SMa2287 (NP_436477.2) on pSymA plus SM_b20494 (NP_437016.1) and SM_b21434 (NP_437803.1) on pSymB are not well-studied, and had weak (SM_b20494) or undetectable effects in a plasmid insertion mutagenesis screen compared to the named *lsr*A and *lsr*B (74). This class of loci is well-known to control expression of genes for symbiosis, both mutualistic and pathogenic (75). Beyond those discovered in knockdown studies, our results suggest additional symbiotic roles for natural variation at these *lys*R regulators in *E. meliloti*. Interestingly, one metabolic process gene (*gdh*A: SMa0228/NP_435368.1 on pSymA; **Supp. Dataset S2**), part of one bacterial pathway for assimilation of ammonium into glutamate (76), was identified in a comparative genomics study of five *Ensifer* (formerly *Sinorhizobium*) species as specific to *E. meliloti* (77). The role of *gdh*A in rhizobial symbiosis is not well-known, though interestingly it was found to increase ammonium assimilation when the *E. coli* copy was expressed transgenically in tobacco (78).

Universal associations highlight transport functions and secretion systems. Despite these layers of context-dependency, we did find significant main effects of strain for all phenotypes (**Table 1**). Concomitantly we resolved a number of loci that were consistently associated with shoot biomass, being mapped in either three experiments (55 nearly-universal genes) or even all four experiments (5 universal genes) (**Fig. 1**). At the genomic and gene-levels, the set of 60 universal/nearly-universal genes were split between pSymA and pSymB (38 and 22 loci, respectively; **Fig. 2** mauve dots; **Supp. Dataset S2**) and featured marginally-enriched INTERPRO terms for "Tetratricopeptide-like helical" ($p < 0.001$) and "Tetratricopeptide repeat-containing domain" ($p = 0.00160$) as well as UNIPROT keywords "Transmembrane" ($p = 0.0190$) and "Transmembrane helix" ($p = 0.0407$), though none of these terms were significant after FDR-correction (**Supp. Dataset S5**).

Of the five truly universal genes (mapped in all 4 experiments; **Supp. Dataset S2**), most do not have known functions in symbiosis. This includes a *cax* gene (SMa0675/NP_435603.2) putatively involved in calcium/proton exchange. Though *cax* genes are widespread in bacteria and eukaryotes (79), and the importance of calcium both in nodule establishment and trade of benefits is known (80, 81), it is difficult to hypothesize on the function of this particular gene or its genetic variants in symbiosis currently. Given their as-yet unknown functions and lack of context-dependency in our studies, the five universal candidates might hold the most potential for novel functional information and consistent phenotypic effects, which might make them ideal candidates both for validation and for symbiosis improvement.

Like the five universal genes, the "nearly-universal" set of genes associated with

bioRχiv Submission Template bioRχiv Submission Template bioRχiv Submission Template bioRχiv Submission Template bioRχiv Submission Template bioRχiv Submission Template bioRχiv Submission Template

shoot biomass in three (of four) experiments highlights the existence of segregating natural variation in a number of interesting metabolic pathways, only some of which have established roles in symbiosis. We found five loci annotated as involved in transmembrane transport (**Supp. Dataset S2**), including *kdp*A (SMa2333/NP_436501.1), *pot*E (SMa0678/NP_435605.1), and *msb*A1 (SM_b20813/NP_437093.2) – in addition to the nodulation protein *glm*S/*nod*M (SMa0878/NP_435728.1) and the universally-associated *cax* transporter (discussed above). The role of potassium transporters such as *kdp*A in osmoregulation during symbiosis is not well understood (82). The *pot*E locus codes for a putrescine/ornithine antiporter, while another nearby nearly-universal locus (SMa0682/NP_435607.4) is a predicted amino acid decarboxylase in the putrescine biosynthesis pathway, potentially suggesting a role for variation in putrescine metabolism (known to vary in *E. meliloti*; Epstein et al. 45) in symbiotic partner quality (45, 83).

We additionally compared our consistent (universal and nearly-universal) candidate gene lists with GWAS associations from other research groups in different genomic backgrounds (e.g., 45, 66), and discovered important roles for natural variation in rhizobial glucosamine processing, T4SS transferase loci (*tra*A and *tra*G), and a handful of others (**Supp. Results**; **Supp. Dataset S2**) in determining symbiotic partner quality in nature.

DISCUSSION

Understanding our symbiotic world requires a genetically-accurate appreciation of the symbiotic extended phenotypes upon which selection acts. While evolutionary ecology has long recognized the importance of genetic variation in symbiosis while ignoring the underlying mechanisms, functional geneticists have traditionally resolved mechanisms without taking into account natural variation. Synthesis of these two perspectives has started to resolve ecologically-relevant quantitative variation at the nucleotide level (84, 46, 85, 60, 45, 47). Here we quantify multiple symbiotic extended phenotypes in four mapping experiments using a model plant-microbe symbiosis and find that the genetic architecture of symbiotic partner quality is complex, underlain by networks of numerous interacting loci and environmental-dependence. We find that some loci in the microbial symbiont have strong and consistent effects on host growth across environments, contributing to the overall differences in mutualistic partner quality that have been the focus of many empirical and theoretical studies of mutualism to date (reviewed by 86, 87, 88, 40, 89). Nonetheless, the vast majority of loci identified in our study were significantly associated with variation in partner quality in specific environments (G $\times$ E effects), or with specific host genotypes (G $\times$ G effects). We first discuss the roles of environmentally-dependent loci, versus universal loci that are found consistently. Next we discuss the coevolutionary implications of genotype-dependence (G x G interactions), then wrap up with a call for further synthesis with metabolic network models towards systems genetics of symbiosis.

Environmental context-dependency in the G→P map of symbiosis. Ecological effects of context-dependency in mutualism have been recognized for a long time, i.e., traits and mutualism benefits often shift across environmental conditions such as nutrient availability or light environments (90, 91, 92), although not ubiquitously for all traits (e.g., 93, 94). More recent studies have begun to document the evolutionary changes that can result from these ecological effects, e.g., divergence of host and/or symbiont symbiosis traits across strong ecological gradients (95, 96, 59, 97, 98). Evolutionary change in response to environments implies that the loci underlying selected traits have differential effects on fitness across environments. Here we identify the loci that generate important trait variation both within and among environments, the

bioRχiv Submission Template bioRχiv Submission Template bioRχiv Submission Template bioRχiv Submission Template bioRχiv Submission Template bioRχiv Submission Template bioRχiv Submission Template

trait variation upon which selection acts in nature.

The majority of context-dependent partner quality genes we identified might be viewed much like the conditionally-neutral variation so often found in studies of local adaptation (99, 100, 101, 102, 103), contributing strongly to variation in partner quality in some contexts but having a range of weaker effects (both in the same or opposing direction) in another context. For example, by experimentally-evolving strains of *E. meliloti* on five *M. truncatula* lines, Batstone et al. (66) found that local adaptation was largely governed by conditional neutrality (beneficial on local host, neutral on non-local hosts) or mildly deleterious effects on non-local hosts, likely due to drift in the local context. Yet, in nature where rhizobium population sizes are much larger and more diverse, and gene flow is present, the extent to which local adaptation occurs has rarely been tested but might be unlikely (28, 104, 105), with the exception of populations differentiated by strong ecological gradients (e.g., 95). Moreover, the host genotypes used in our study, DZA and A17, are unlikely to share an evolutionary history with our strains, and so it remains unclear whether stronger trade-offs (and less conditional neutrality) would be present if our strains shared an evolutionary history with the host lines being tested.

Despite widespread conditional neutrality, a handful of interesting variants had strong effects on host growth, but in *opposing directions* across experiments within a single host genetic background. These sorts of antagonistic effects can favour different variants in different environments, and thus, potentially help explain the maintenance of mutualism variation in nature (106, 88, 107, 108). Nevertheless we note that these sorts of G $\times$ E variants were rare in our study, despite strong rank-order effects among strain means at the organismal level (**Table 2**); moreover, because our "environments" were simply different greenhouse experiments, relating such antagonistic effects to adaptation in the wild will require the type of *in situ* studies that are common in plants (e.g., 100, 97, 109) but more difficult in soil microbes. We nevertheless found several genes and pathways that are ideal for functional follow-up studies aimed at identifying consistent associations, or loci which might benefit from "fine-tuning" symbiotic benefits towards improving plant health. The strengths of GWAS (capturing genetic variation, ecological relevance) also lead to weaknesses (imprecision due to confounding population structure, false negatives and false positives). Thus our strongest recommendations for functional hypotheses for validation in follow up studies are the universal genes identified here that overlap with candidate genes identified in separate GWAS using different genomic backgrounds and environments (e.g., 45, 66).

Overall we find that the loci underlying quantitative variation in symbiotic extended phenotypes often (but not always) depend on the environment, and therefore that a nuanced understanding of how complex traits interact with environmental variables will be necessary for many of the lofty goals in plant microbiome and symbiosis research (9, 35). This point has been made before (110), as the presence of G $\times$ E as studied at the phenotypic level has been recognized for decades; what is novel here is our ability to interrogate this variation at the genomic level and for multiple host lines (see below).

Coevolutionary implications of genotype-dependence. Previous mapping efforts in the legume-rhizobium system have focused on the HapMap collections, which maximize diversity using a range-wide sample. Our study focuses on the segregating natural variation at a smaller geographic scale, a scale at which pSymA and pSymB segregate (105); thus the G $\times$ G-driven variation we find here would be available to local evolutionary and/or coevolutionary processes. G $\times$ G interactions for fitness outcomes have long been of interest in the legume-rhizobium symbiosis (25, 111, 28, 95, 112)

bioRχiv Submission Template bioRχiv Submission Template bioRχiv Submission Template bioRχiv Submission Template bioRχiv Submission Template bioRχiv Submission Template bioRχiv Submission Template

and other interactions (113, 114, 115) because such statistical interactions generate the fitness variation that drives coevolution, but also have implications for breeding and agricultural production whereby the functional effects of symbiont variation depend on the crop genotype (116, 117). Recent molecular genetic and transcriptomic approaches on a handful of genotypes have begun to resolve the mechanistic underpinnings of G × G (118, 119, 120, 121, 122, 123), while biparental or GWAS mapping approaches (124, 46, 45) provide broader insight into the genetic architecture underlying G × G (i.e., the number, average effect size, and consistency of loci). The picture emerging from ours and others' studies is that G × G, like symbiotic partner quality itself, has a complex, polygenic basis and will require both statistically sophisticated and metabolically-informed models to unravel.

Symbiotic extended phenotypes as quantitative traits. In the age of rapid microbiome sequencing and expanding efforts to characterize the loci in plant genomes that contribute to microbiome variation among cultivars or genotypes (e.g., rice, *Lotus*, *Medicago*), our results present an important juxtaposition, as the abundant and context-dependent genetic variation characterized in detail here occurs within a set of 191 strains with > 98% average nucleotide identity (well above the typical threshold for delineating and enumerating operational taxonomic units, or OTUs, in metagenomic studies). At the same time, functional genetic studies have made much progress identifying loci critical to symbiosis establishment and downstream processes by creating knock-out or knock-down mutants and comparing their associated symbiotic phenotypes to a wildtype strain (e.g., *dnf* mutants in legumes, Ané et al. 125; fix+/fix- mutants of rhizobia, Wheatley et al. 126), but these loci are often viewed as on-or-off switches for symbiosis more generally, or cooperation more specifically in models of mutualism theory (127, 128, 129, 130). Our study demonstrates that the vast majority of loci within the symbiont genome act more like dials than on-and-off switches, generating the quantitative variation in symbiotic extended phenotypes observed in nature.

While our approach allows us to zero-in on particular loci underlying G × E and G × G interactions, *in silico* modelling of both plant (131) and rhizobium (132) metabolism that links together genetic information with metabolic pathways could then be used to simulate key symbiotic processes under a wide range of conditions (133). Ultimately combining transcriptomic, genomic, and metabolomic datasets will be required for a synthetic understanding of how nucleotide variation percolates up through shared symbiotic metabolic networks (134, 135, 17). Efforts to reintegrate research on symbiosis genetics and (co)evolution with plant-microbiome work (reviewed in 136, 37) will be fruitful in revealing additional intraspecific variation driving patterns of genotype-dependence and coevolution and resolving mechanisms of host control of the microbiome.

MATERIALS AND METHODS

Full details are available in the Supplemental Materials (**Supp. Methods**). We performed four greenhouse experiments to estimate partner quality phenotypes in *E. meliloti*. In each experiment, plants from one of two host lines (either A17 or DZA) were grown in single inoculation with each of 191 *E. meliloti* strains, with three to four replicates per strain per experiment (six to eight total replicates for each plant line x strain combination, N = 2,825 plants total). Experiments were planted in 2018, in March (I: DZA), May (II: A17), Sept (III: DZA), and Nov (IV: A17). Uninoculated controls (40 per experiment) were included to gauge contamination, which was minimal overall, and limited to the first two experiments (**Supp. Fig. S10**). We measured multiple proxies of partner quality, namely leaf chlorophyll A content, plant height, number of

bioRχiv Submission Template bioRχiv Submission Template bioRχiv Submission Template bioRχiv Submission Template bioRχiv Submission Template bioRχiv Submission Template bioRχiv Submission Template

leaves, and above-ground dried shoot biomass, although we focus on the latter in the main text (see Supplemental Materials for all others). We conducted multiple phenotypic analyses to determine how much variation in partner quality was due to strain, experiment, and the interaction of both, among other questions.

We sequenced the entire genomes of all 191 *E. meliloti* strains, called single nucleotide polymorphisms (SNPs, henceforth referred to as variants), and performed genome-wide association tests that accounted for rhizobium population structure and included only unlinked variants. We determined which loci were significantly associated with partner quality using a permutation method, and binned these loci into three categories based on the context-dependency of their phenotypic effects, and thus, their contribution to the layers of the G→P map for each of our symbiotic extended phenotypes. First,"nearly-universal genes" were those found to have significant effects in at least three of the four experiments for a particular trait ("universal genes" were mapped in all four experiments). Second, we used a conservative approach to call "G × G genes" as those mapped in both experiments for one host genotype but neither of the experiments for the other host genotype (i.e., "DZA G × G" genes were significant in both experiments I and III with DZA but neither II nor IV with host A17). Third were genes significantly associated with partner quality in a single experiment, and never in another (i.e., "G × E" genes). Finally, we conducted candidate gene functional analyses to understand how loci within different categories differed from one another, or whether they were part of the same networks/metabolic pathways.

Data Availability. Strains and plant lines are available upon request. All raw data and code to reproduce analyses will be made available on GitHub upon publication. Once raw sequence reads and assemblies are archived and made available on NCBI, accession numbers will be added here as well.

SUPPLEMENTAL MATERIAL

Includes detailed methods, additional results, seven (7) supplementary datasets and twelve (12) supplementary figures. Additionally provides legends for datasets and figures. The manuscript doc and all supplemental datasets can also be accessed from bioRχiv doi https://doi.org/10.1101/2021.08.03.454976.

ACKNOWLEDGMENTS

We thank greenhouse staff (esp. Debbie Black). We acknowledge funding from the National Science Foundation (IOS-1645875 and NPGI-1401864), a Carl R. Woese Institute for Genomic Biology postdoctoral fellowship to R.T. Batstone, strain sequencing by Joint Genome Institute (CSP-1223795), as well as analytical advice from B. Epstein.

REFERENCES

1. **Klironomos JN**. 2003. Variation in plant response to native and exotic arbuscular mycorrhizal fungi. Ecology 84 (9):2292–2301.
2. **Oliver KM, Moran NA, Hunter MS**. 2005. Variation in resistance to parasitism in aphids is due to symbionts not host genotype. Proc Natl Acad Sci 102 (36):12795–12800.
3. **Ridaura VK, Faith JJ, Rey FE, Cheng J, Duncan AE, Kau AL, Griffin NW, Lombard V, Henrissat B, Bain JR, et al.**. 2013. Gut microbiota from twins discordant for obesity modulate metabolism in mice. Science 341 (6150).
4. **Brock DA, Jones K, Queller DC, Strassmann JE**. 2016. Which phenotypic traits of Dictyostelium discoideum farmers are conferred by their bacterial symbionts? Symbiosis 68 (1-3):39–48.
5. **Gilbert JA, Lynch SV**. 2019. Community ecology as a framework for human microbiome research. Nat Med 25 (6):884–889.
6. **O'Brien AM, Jack CN, Friesen ML, Frederickson ME**. 2021. Whose trait is it anyways? Coevolution of joint phenotypes and genetic architecture in mutualisms. Proc Royal Soc B 288 (1942):20202483.
7. **Afkhami ME, Friesen ML, Stinchcombe JR**. 2021. Multiple Mutualism Effects generate synergistic selection and strengthen fitness alignment in the interaction between legumes, rhizobia and mycorrhizal fungi. Ecol Lett .
8. **Brundrett MC**. 2002. Coevolution of roots and mycorrhizas of land plants. New Phytol 154 (2):275–304.
9. **Friesen ML, Porter SS, Stark SC, von Wettberg EJ, Sachs JL,**

bioRχiv Submission Template bioRχiv Submission Template bioRχiv Submission Template bioRχiv Submission Template bioRχiv Submission Template bioRχiv Submission Template bioRχiv Submission Template

Martinez-Romero E. 2011. Microbially mediated plant functional traits. Annu Rev Ecol Evol Syst 42:23–46.
10. **Hurst GD**. 2017. Extended genomes: symbiosis and evolution. Interface Focus 7 (5):20170001.
11. **Hawkes CV, Bull JJ, Lau JA**. 2020. Symbiosis and stress: how plant microbiomes affect host evolution. Philos Trans Royal Soc B 375 (1808):20190590.
12. **Moeller AH, Sanders JG**. 2020. Roles of the gut microbiota in the adaptive evolution of mammalian species. Philos Trans Royal Soc B 375 (1808):20190597.
13. **Hansen TF**. 2006. The evolution of genetic architecture. Annu Rev. Ecol. Evol. Syst. 37:123–157.
14. **Orgogozo V, Morizot B, Martin A**. 2015. The differential view of genotype–phenotype relationships. Front Genet 6:179.
15. **Mackay TF, Huang W**. 2018. Charting the genotype–phenotype map: lessons from the Drosophila melanogaster Genetic Reference Panel. Wiley Interdiscip Rev Dev Biol 7 (1):e289.
16. **Checcucci A, diCenzo GC, Ghini V, Bazzicalupo M, Becker A, Decorosi F, Döhlemann J, Fagorzi C, Finan TM, Fondi M, et al.**. 2018. Creation and characterization of a genomically hybrid strain in the nitrogen-fixing symbiotic bacterium *Sinorhizobium meliloti*. ACS Synth Biol 7 (10):2365–2378.
17. **Marshall-Colón A, Kliebenstein DJ**. 2019. Plant networks as traits and hypotheses: moving beyond description. Trends Plant Sci 24 (9):840–852.
18. **Cheverud JM**. 1982. Phenotypic, genetic, and environmental morphological integration in the cranium. Evolution p 499–516.
19. **Cheverud JM**. 1996. Developmental integration and the evolution of pleiotropy. Am Zoöl 36 (1):44–50.
20. **Hansen TF**. 2013. Why epistasis is important for selection and adaptation. Evolution 67 (12):3501–3511.
21. **Lee SH, Ripke S, Neale BM, Faraone SV, Purcell SM, Perlis RH, Mowry BJ, Thapar A, Goddard ME, Witte JS, et al.**. 2013. Genetic relationship between five psychiatric disorders estimated from genome-wide SNPs. Nat Genet 45 (9):984–995.
22. **Campbell-Staton SC, Cheviron ZA, Rochette N, Catchen J, Losos JB, Edwards SV**. 2017. Winter storms drive rapid phenotypic, regulatory, and genomic shifts in the green anole lizard. Science 357 (6350):495–498.
23. **Saltz JB, Hessel FC, Kelly MW**. 2017. Trait correlations in the genomics era. Trends Ecol & Evol 32 (4):279–290.
24. **Frank S**. 1992. Models of plant-pathogen coevolution. Trends Genet 8 (6):213–219.
25. **Parker MP**. 1995. Plant fitness variation caused by different mutualist genotypes. Ecology 76 (5):1525–1535.
26. **Lambrechts L, Fellous S, Koella JC**. 2006. Coevolutionary interactions between host and parasite genotypes. Trends Parasitol 22 (1):12–16.
27. **Wade MJ**. 2007. The co-evolutionary genetics of ecological communities. Nat Rev Genet 8 (3):185–195.
28. **Heath KD**. 2010. Intergenomic epistasis and coevolutionary constraint in plants and rhizobia. Evolution 64 (5):1446–1458.
29. **Parker BJ, Hrček J, McLean AH, Godfray HCJ**. 2017. Genotype specificity among hosts, pathogens, and beneficial microbes influences the strength of symbiont-mediated protection. Evolution 71 (5):1222–1231.
30. **Piculell BJ, Hoeksema JD, Thompson JN**. 2008. Interactions of biotic and abiotic environmental factors in an ectomycorrhizal symbiosis, and the potential for selection mosaics. BMC Biol 6 (1):1–11.
31. **Heath KD, Stock A, Stinchcombe J**. 2010. Mutualism variation in the nodulation response to nitrate. J Evol Biol 23 (11):2494–2500.
32. **Wendling CC, Fabritzek AG, Wegner KM**. 2017. Population-specific genotype x genotype x environment interactions in bacterial disease of early life stages of pacific oyster larvae. Evol Appl 10 (4):338–347.
33. **Thompson JN**. 2005. The geographic mosaic of coevolution. University of Chicago Press.
34. **Thompson JN**. 2009. The coevolutionary process. University of Chicago press.
35. **Busby PE, Soman C, Wagner MR, Friesen ML, Kremer J, Bennett A, Morsy M, Eisen JA, Leach JE, Dangl JL**. 2017. Research priorities for harnessing plant microbiomes in sustainable agriculture. PLoS Biol 15 (3):e2001793.
36. **Porter SS, Sachs JL**. 2020. Agriculture and the disruption of plant–microbial symbiosis. Trends Ecol & Evol 35 (5):426–439.
37. **Batstone RT**. 2021. Genomes within Genomes: nested symbiosis and its implications for plant evolution. New Phytol (in review).
38. **Cook DR**. 1999. *Medicago truncatula*–a model in the making! Curr Opin Plant Biol 2 (4):301–304.
39. **Heath KD, Grillo MA**. 2016. Rhizobia: tractable models for bacterial evolutionary ecology: Models for bacterial evolutionary ecology. Environ Microbiol 18 (12).
40. **Sachs JL, Quides KW, Wendlandt CE**. 2018. Legumes versus rhizobia: a model for ongoing conflict in symbiosis. New Phytol 219 (4):1199–1206.
41. **diCenzo GC, Zamani M, Checcucci A, Fondi M, Griffitts JS, Finan TM, Mengoni A**. 2019. Multidisciplinary approaches for studying rhizobium–legume symbioses. Can J Microbiol 65 (1):1–33.
42. **Burghardt LT**. 2020. Evolving together, evolving apart: measuring the fitness of rhizobial bacteria in and out of symbiosis with leguminous plants. New Phytol 228 (1):28–34.
43. **Young ND, Cannon SB, Sato S, Kim D, Cook DR, Town CD, Roe BA, Tabata S**. 2005. Sequencing the genespaces of *Medicago truncatula* and *Lotus japonicus*. Plant Physiol 137 (4):1174–1181.
44. **Epstein B, Branca A, Mudge J, Bharti AK, Briskine R, Farmer AD, Sugawara M, Young ND, Sadowsky MJ, Tiffin P**. 08 2012. Population Genomics of the Facultatively Mutualistic Bacteria *Sinorhizobium meliloti* and *S. medicae*. PLoS Genet 8:1–10. doi: 10.1371/journal.pgen.1002868.
45. **Epstein B, Abou-Shanab RA, Shamseldin A, Taylor MR, Guhlin J, Burghardt LT, Nelson M, Sadowsky MJ, Tiffin P**. 2018. Genome-wide association analyses in the model Rhizobium *Ensifer meliloti*. MSphere 3 (5).
46. **Stanton-Geddes J, Paape T, Epstein B, Briskine R, Yoder J, Mudge J, Bharti AK, Farmer AD, Zhou P, Denny R, et al.**. 2013. Candidate genes and genetic architecture of symbiotic and agronomic traits revealed by whole-genome, sequence-based association genetics in *Medicago truncatula*. PloS One 8 (5):e65688.
47. **Burghardt LT, Epstein B, Guhlin J, Nelson MS, Taylor MR, Young ND, Sadowsky MJ, Tiffin P**. 2018. Select and resequence reveals relative fitness of bacteria in symbiotic and free-living environments. Proc Natl Acad Sci 115 (10):2425–2430.
48. **Graham PH, Vance CP**. 2003. Legumes: importance and constraints to greater use. Plant Physiol 131 (3):872–877.
49. **Foyer CH, Lam HM, Nguyen HT, Siddique KH, Varshney RK, Colmer TD, Cowling W, Bramley H, Mori TA, Hodgson JM, et al.**. 2016. Neglecting legumes has compromised human health and sustainable food production. Nat Plants 2 (8):1–10.
50. **Fustec J, Lesuffleur F, Mahieu S, Cliquet JB**. 2010. Nitrogen rhizodeposition of legumes. A review. Agron for Sustain Dev 30 (1):57–66.
51. **Duchene O, Vian JF, Celette F**. 2017. Intercropping with legume for agroecological cropping systems: Complementarity and facilitation processes and the importance of soil microorganisms. A review. Agric

bioRχiv Submission Template bioRχiv Submission Template bioRχiv Submission Template bioRχiv Submission Template bioRχiv Submission Template bioRχiv Submission Template bioRχiv Submission Template

Ecosyst & Environ 240:148–161.
52. **Harrison PW, Lower RP, Kim NK, Young JPW**. 2010. Introducing the bacterial 'chromid': not a chromosome, not a plasmid. Trends Microbiol 18 (4):141–148.
53. **Young ND, Zhou P, Silverstein KA**. 2016. Exploring structural variants in environmentally sensitive gene families. Curr Opin Plant Biol 30:19–24.
54. **Dicenzo GC, Finan TM**. 2017. The divided bacterial genome: structure, function, and evolution. Microbiol Mol Biol Rev 81 (3):e00019–17.
55. **Misra HS, Maurya GK, Kota S, Charaka VK**. 2018. Maintenance of multipartite genome system and its functional significance in bacteria. J Genet 97 (4):1013–1038.
56. **Cavassim MIA, Moeskjær S, Moslemi C, Fields B, Bachmann A, Vilhjálmsson BJ, Schierup MH, Young JPW, Andersen SU**. 2020. Symbiosis genes show a unique pattern of introgression and selection within a Rhizobium leguminosarum species complex. Microb Genom 6 (4).
57. **Nelson M, Guhlin J, Epstein B, Tiffin P, Sadowsky MJ**. 2018. The complete replicons of 16 Ensifer meliloti strains offer insights into intra-and inter-replicon gene transfer, transposon-associated loci, and repeat elements. Microb Genom 4 (5).
58. **Epstein B, Tiffin P**. 2021. Comparative genomics reveals high rates of horizontal transfer and strong purifying selection on rhizobial symbiosis genes. Proc Royal Soc B 288 (1942):20201804.
59. **Klinger CR, Lau JA, Heath KD**. 2016. Ecological genomics of mutualism decline in nitrogen-fixing bacteria. Proc Royal Soc B 283 (1826):20152563.
60. **Porter SS, Chang PL, Conow CA, Dunham JP, Friesen ML**. 2017. Association mapping reveals novel serpentine adaptation gene clusters in a population of symbiotic Mesorhizobium. The ISME J 11 (1):248–262.
61. **Power RA, Parkhill J, de Oliveira T**. 2017. Microbial genome-wide association studies: lessons from human GWAS. Nat Rev Genet 18 (1):41–50.
62. **Wang D, Yang S, Tang F, Zhu H**. 2012. Symbiosis specificity in the legume–rhizobial mutualism. Cell Microbiol 14 (3):334–342.
63. **Roy S, Liu W, Nandety RS, Crook A, Mysore KS, Pislariu CI, Frugoli J, Dickstein R, Udvardi MK**. 2020. Celebrating 20 years of genetic discoveries in legume nodulation and symbiotic nitrogen fixation. The Plant Cell 32 (1):15–41.
64. **diCenzo GC, Tesi M, Pfau T, Mengoni A, Fondi M**. 2020. Genome-scale metabolic reconstruction of the symbiosis between a leguminous plant and a nitrogen-fixing bacterium. Nat Commun 11 (1):1–11.
65. **Porter SS, Faber-Hammond J, Montoya AP, Friesen ML, Sackos C**. 2019. Dynamic genomic architecture of mutualistic cooperation in a wild population of Mesorhizobium. The ISME J 13 (2):301–315.
66. **Batstone RT, O'Brien AM, Harrison TL, Frederickson ME**. 2020. Experimental evolution makes microbes more cooperative with their local host genotype. Science 370 (6515):476–478.
67. **Becker A, Kleickmann A, Küster H, Keller M, Arnold W, Pühler A**. 1993. Analysis of the *Rhizobium meliloti* genes exoU, exoV, exoW, exoT, and exoI involved in exopolysaccharide biosynthesis and nodule invasion: exoU and exoW probably encode glucosyltransferases. Mol Plant-Microbe Interactions: MPMI 6 (6):735–744.
68. **Reuber TL, Walker GC**. 1993. Biosynthesis of succinoglycan, a symbiotically important exopolysaccharide of *Rhizobium meliloti*. Cell 74 (2):269–280.
69. **Nogales J, Muñoz S, Olivares J, Sanjuán J**. 2006. *Sinorhizobium meliloti* genes involved in tolerance to the antimicrobial peptide protamine. FEMS Microbiol Lett 264 (2):160–167.
70. **Mendis HC, Madzima TF, Queiroux C, Jones KM**. 2016. Function of succinoglycan polysaccharide in *Sinorhizobium meliloti* host plant invasion depends on succinylation, not molecular weight. MBio 7 (3):e00606–16.
71. **Copeland PR**. 2005. Making sense of nonsense: the evolution of selenocysteine usage in proteins. Genome Biol 6 (6):1–5.
72. **Peng T, Lin J, Xu YZ, Zhang Y**. 2016. Comparative genomics reveals new evolutionary and ecological patterns of selenium utilization in bacteria. The ISME J 10 (8):2048–2059.
73. **Wells M, Stolz JF**. 2020. Microbial selenium metabolism: a brief history, biogeochemistry and ecophysiology. FEMS Microbiol Ecol 96 (12):fiaa209.
74. **Luo L, Yao SY, Becker A, Rüberg S, Yu GQ, Zhu JB, Cheng HP**. 2005. Two new *Sinorhizobium meliloti Lys*R-type transcriptional regulators required for nodulation. J Bacteriol 187 (13):4562–4572.
75. **Schell MA**. 1993. Molecular biology of the *Lys*R family of transcriptional regulators. Annu Rev Microbiol 47 (1):597–626.
76. **Merrick M, Edwards R**. 1995. Nitrogen control in bacteria. Microbiol Rev 59 (4):604–622.
77. **Sugawara M, Epstein B, Badgley BD, Unno T, Xu L, Reese J, Gyaneshwar P, Denny R, Mudge J, Bharti AK, et al.**. 2013. Comparative genomics of the core and accessory genomes of 48 *Sinorhizobium* strains comprising five genospecies. Genome Biol 14 (2):1–20.
78. **Ameziane R, Bernhard K, Lightfoot D**. 2000. Expression of the bacterial *gdh*A gene encoding a NADPH glutamate dehydrogenase in tobacco affects plant growth and development. Plant Soil 221 (1):47–57.
79. **Shigaki T, Rees I, Nakhleh L, Hirschi K**. 2006. Identification of three distinct phylogenetic groups of CAX cation/proton antiporters. J Mol Evol 63 (6):815–825.
80. **Oldroyd GE, Downie JA**. 2004. Calcium, kinases and nodulation signalling in legumes. Nat Rev Mol Cell Biol 5 (7):566–576.
81. **Clarke VC, Loughlin PC, Day DA, Smith P**. 2014. Transport processes of the legume symbiosome membrane. Front Plant Sci 5:699.
82. **Domínguez-Ferreras A, Muñoz S, Olivares J, Soto MJ, Sanjuán J**. 2009. Role of potassium uptake systems in *Sinorhizobium meliloti* osmoadaptation and symbiotic performance. J Bacteriol 191 (7):2133–2143.
83. **Becerra-Rivera VA, Dunn MF**. 2019. Polyamine biosynthesis and biological roles in rhizobia. FEMS Microbiol Lett 366 (7):fnz084.
84. **Branca A, Paape TD, Zhou P, Briskine R, Farmer AD, Mudge J, Bharti AK, Woodward JE, May GD, Gentzbittel L, et al.**. 2011. Whole-genome nucleotide diversity, recombination, and linkage disequilibrium in the model legume *Medicago truncatula*. Proc Natl Acad Sci 108 (42):E864–E870.
85. **Friesen ML, von Wettberg EJ, Badri M, Moriuchi KS, Barhoumi F, Chang PL, Cuellar-Ortiz S, Cordeiro MA, Vu WT, Arraouadi S, et al.**. 2014. The ecological genomic basis of salinity adaptation in Tunisian *Medicago truncatula*. BMC Genom 15 (1):1160.
86. **Denison RF**. 2000. Legume sanctions and the evolution of symbiotic cooperation by rhizobia. The Am Nat 156 (6):567–576.
87. **Simms EL, Taylor DL**. 2002. Partner choice in nitrogen-fixation mutualisms of legumes and rhizobia. Integr Comp Biol 42 (2):369–380.
88. **Heath KD, Stinchcombe JR**. 2014. Explaining mutualism variation: a new evolutionary paradox? Evolution 68 (2):309–317.
89. **Stoy KS, Gibson AK, Gerardo NM, Morran LT**. 2020. A need to consider the evolutionary genetics of host–symbiont mutualisms. J Evol Biol 33 (12):1656–1668.
90. **Chamberlain SA, Bronstein JL, Rudgers JA**. 2014. How context dependent are species interactions? Ecol Lett 17 (7):881–890.

bioRχiv Submission Template bioRχiv Submission Template bioRχiv Submission Template bioRχiv Submission Template bioRχiv Submission Template bioRχiv Submission Template bioRχiv Submission Template

91. **Bronstein JL**. 2015. Mutualism. Oxford University Press, USA.
92. **Hoeksema JD, Bruna EM**. 2015. Context-Dependent Outcomes of Mutualistic Interactions, p 181–202. *In* Bronstein JL (ed), Mutualism. Oxford University Press, Oxford, UK.
93. **Regus JU, Gano KA, Hollowell AC, Sachs JL**. 2014. Efficiency of partner choice and sanctions in Lotus is not altered by nitrogen fertilization. Proc Royal Soc B: Biol Sci 281 (1781):20132587.
94. **Grillo MA, Stinchcombe JR, Heath KD**. 2016. Nitrogen addition does not influence pre-infection partner choice in the legume–rhizobium symbiosis. Am J Bot 103 (10):1763–1770.
95. **Porter SS, Stanton ML, Rice KJ**. 2011. Mutualism and adaptive divergence: co-invasion of a heterogeneous grassland by an exotic legume-rhizobium symbiosis. PloS One 6 (12):e27935.
96. **Weese DJ, Heath KD, Dentinger BT, Lau JA**. 2015. Long-term nitrogen addition causes the evolution of less-cooperative mutualists. Evolution 69 (3):631–642.
97. **Rúa MA, Antoninka A, Antunes PM, Chaudhary VB, Gehring C, Lamit LJ, Piculell BJ, Bever JD, Zabinski C, Meadow JF, et al.**. 2016. Home-field advantage? Evidence of local adaptation among plants, soil, and arbuscular mycorrhizal fungi through meta-analysis. BMC Evol Biol 16 (1):1–15.
98. **Piculell BJ, José Martínez-García P, Nelson CD, Hoeksema JD**. 2019. Association mapping of ectomycorrhizal traits in loblolly pine (Pinus taeda L.). Mol Ecol 28 (8):2088–2099.
99. **Anderson JT, Willis JH, Mitchell-Olds T**. 2011. Evolutionary genetics of plant adaptation. Trends Genet 27 (7):258–266.
100. **Anderson JT, Lee CR, Rushworth CA, Colautti RI, Mitchell-Olds T**. 2013. Genetic trade-offs and conditional neutrality contribute to local adaptation. Mol Ecol 22 (3):699–708.
101. **Des Marais DL, Hernandez KM, Juenger TE**. 2013. Genotype-by-environment interaction and plasticity: exploring genomic responses of plants to the abiotic environment. Annu Rev Ecol Evol Syst 44:5–29.
102. **Wadgymar SM, Lowry DB, Gould BA, Byron CN, Mactavish RM, Anderson JT**. 2017. Identifying targets and agents of selection: innovative methods to evaluate the processes that contribute to local adaptation. Methods Ecol Evol 8 (6):738–749.
103. **Mee JA, Yeaman S**. 2019. Unpacking conditional neutrality: genomic signatures of selection on conditionally beneficial and conditionally deleterious mutations. The Am Nat 194 (4):529–540.
104. **Harrison TL, Wood CW, Borges IL, Stinchcombe JR**. 2017. No evidence for adaptation to local rhizobial mutualists in the legume *Medicago lupulina*. Ecol Evol 7 (12):4367–4376.
105. **Riley A, Grillo M, Epstein B, Tiffin P, Heath K**. 2021. Partners in space: Discordant population structure between legume hosts and rhizobium symbionts in their native range .
106. **Frederickson ME**. 2013. Rethinking mutualism stability: cheaters and the evolution of sanctions. The Q Rev Biol 88 (4):269–295.
107. **Pahua V, Stokes P, Hollowell A, Regus J, Gano-Cohen K, Wendlandt C, Quides K, Lyu J, Sachs J**. 2018. Fitness variation among host species and the paradox of ineffective rhizobia. J Evol Biol 31 (4):599–610.
108. **Vaidya P, Stinchcombe JR**. 2020. The Potential for Genotype-by-Environment Interactions to Maintain Genetic Variation in a Model Legume–Rhizobia Mutualism. Plant Commun 1 (6):100114.
109. **Popovic D, Lowry DB**. 2020. Contrasting environmental factors drive local adaptation at opposite ends of an environmental gradient in the yellow monkeyflower (Mimulus guttatus). Am J Bot 107 (2):298–307.
110. **Mackay TF, Stone EA, Ayroles JF**. 2009. The genetics of quantitative traits: challenges and prospects. Nat Rev Genet 10 (8):565–577.
111. **Burdon J, Thrall P**. 1999. Spatial and temporal patterns in coevolving plant and pathogen associations. The Am Nat 153 (S5):S15–S33.
112. **Barrett LG, Broadhurst LM, Thrall PH**. 2012. Geographic adaptation in plant–soil mutualisms: tests using *Acacia* spp. and rhizobial bacteria. Funct Ecol 26 (2):457–468.
113. **Vale PF, Little TJ**. 2010. CRISPR-mediated phage resistance and the ghost of coevolution past. Proc Royal Soc B 277 (1691):2097–2103.
114. **Hoeksema JD**. 2010. Ongoing coevolution in mycorrhizal interactions. New Phytol 187 (2):286–300.
115. **Chong RA, Moran NA**. 2016. Intraspecific genetic variation in hosts affects regulation of obligate heritable symbionts. Proc Natl Acad Sci 113 (46):13114–13119.
116. **Wallace JG, Rodgers-Melnick E, Buckler ES**. 2018. On the road to breeding 4.0: unraveling the good, the bad, and the boring of crop quantitative genomics. Annu Rev Genet 52:421–444.
117. **Clouse KM, Wagner MR**. 2021. Plant genetics as a tool for manipulating crop microbiomes: Opportunities and challenges. Front Bioeng Biotechnol 9.
118. **Heath KD, Burke PV, Stinchcombe JR**. 2012. Coevolutionary genetic variation in the legume-rhizobium transcriptome. Mol Ecol 21 (19):4735–4747.
119. **Guefrachi I, Nagymihaly M, Pislariu CI, Van de Velde W, Ratet P, Mars M, Udvardi MK, Kondorosi E, Mergaert P, Alunni B**. 2014. Extreme specificity of NCR gene expression in *Medicago truncatula*. BMC Genom 15 (1):1–16.
120. **Burghardt LT, Guhlin J, Chun CL, Liu J, Sadowsky MJ, Stupar RM, Young ND, Tiffin P**. 2017. Transcriptomic basis of genome by genome variation in a legume-rhizobia mutualism. Mol Ecol 26 (21):6122–6135.
121. **Wang Q, Liu J, Zhu H**. 2018. Genetic and molecular mechanisms underlying symbiotic specificity in legume-rhizobium interactions. Front Plant Sci 9:313.
122. **Walker L, Lagunas B, Gifford ML**. 2020. Determinants of host range specificity in legume-rhizobia Symbiosis. Front Microbiol 11:3028.
123. **Fagorzi C, Bacci G, Huang R, Cangioli L, Checcucci A, Fini M, Perrin E, Natali C, diCenzo GC, Mengoni A**. 2021. Nonadditive Transcriptomic Signatures of Genotype-by-Genotype Interactions during the Initiation of Plant-Rhizobium Symbiosis. MSystems 6 (1):e00974–20.
124. **Gorton AJ, Heath KD, Pilet-Nayel ML, Baranger A, Stinchcombe JR**. 2012. Mapping the genetic basis of symbiotic variation in legume-rhizobium interactions in *Medicago truncatula*. G3: Genes| Genomes| Genet 2 (11):1291–1303.
125. **Ané JM, Kiss GB, Riely BK, Penmetsa RV, Oldroyd GE, Ayax C, Lévy J, Debellé F, Baek JM, Kalo P, et al.**. 2004. *Medicago truncatula dmi*1 required for bacterial and fungal symbioses in legumes. Science 303 (5662):1364–1367.
126. **Wheatley RM, Ford BL, Li L, Aroney ST, Knights HE, Ledermann R, East AK, Ramachandran VK, Poole PS**. 2020. Lifestyle adaptations of Rhizobium from rhizosphere to symbiosis. Proc Natl Acad Sci 117 (38):23823–23834.
127. **Bull JJ, Rice W**. 1991. Distinguishing mechanisms for the evolution of co-operation. J Theor Biol 149 (1):63–74.
128. **West S, Kiers ET, Pen I, Denison R**. 2002. Sanctions and mutualism stability: when should less beneficial mutualists be tolerated? J Evol Biol 15 (5):830–837.
129. **West SA, Kiers ET, Simms EL, Denison RF**. 2002. Sanctions and mutualism stability: why do rhizobia fix nitrogen? Proc Royal Soc B 269 (1492):685–694.
130. **Foster KR, Kokko H**. 2006. Cheating can stabilize cooperation in mutualisms. Proc Royal Soc B 273 (1598):2233–2239.
131. **Pfau T, Christian N, Masakapalli SK, Sweetlove LJ, Poolman MG, Ebenhöh O**. 2018. The intertwined metabolism during symbiotic ni-

bioRχiv Submission Template bioRχiv Submission Template bioRχiv Submission Template bioRχiv Submission Template bioRχiv Submission Template bioRχiv Submission Template bioRχiv Submission Template

trogen fixation elucidated by metabolic modelling. Sci Reports 8 (1):1–11.

132. **Checcucci A, Bazzicalupo M, Mengoni A, Viti C, Dziewit L, Finan TM, Galardini M, Fondi M, et al.**. 2016. Metabolic modelling reveals the specialization of secondary replicons for niche adaptation in *Sinorhizobium meliloti*. Nat Commun 7 (1):1–10.
133. **diCenzo GC, Finan TM**. 2018. Techniques for large-scale bacterial genome manipulation and characterization of the mutants with respect to in silico metabolic reconstructions, p 291–314. *In* Metabolic Network Reconstruction and Modeling. Springer.
134. **Civelek M, Lusis AJ**. 2014. Systems genetics approaches to understand complex traits. Nat Rev Genet 15 (1):34–48.
135. **Kliebenstein D**. 2004. Secondary metabolites and plant/environment interactions: a view through *Arabidopsis thaliana* tinged glasses. Plant, Cell & Environ 27 (6):675–684.
136. **Wagner MR**. 2021. Prioritizing host phenotype to understand microbiome heritability in plants. New Phytol (Accepted article).
137. **Tirichine L, de Billy F, Huguet T**. 2000. Mtsym6, a gene conditioning *Sinorhizobium* strain-specific nitrogen fixation in *Medicago truncatula*. Plant Physiol 123 (3):845–852.
138. **Wang Q, Yang S, Liu J, Terecskei K, Ábrahám E, Gombár A, Domonkos Á, Szűcs A, Körmöczi P, Wang T, et al.**. 2017. Host-secreted antimicrobial peptide enforces symbiotic selectivity in *Medicago truncatula*. Proc Natl Acad Sci 114 (26):6854–6859.
139. **Yang S, Wang Q, Fedorova E, Liu J, Qin Q, Zheng Q, Price PA, Pan H, Wang D, Griffitts JS, et al.**. 2017. Microsymbiont discrimination mediated by a host-secreted peptide in *Medicago truncatula*. Proc Natl Acad Sci 114 (26):6848–6853.
140. **Grillo MA, De Mita S, Burke PV, Solórzano-Lowell KL, Heath KD**. 2016. Intrapopulation genomics in a model mutualist: Population structure and candidate symbiosis genes under selection in *Medicago truncatula*. Evolution 70 (12):2704–2717.
141. **Somasegaran P, Hoben HJ**. 1994. Methods in Legume-Rhizobium Technology. *In* Handbook for Rhizobia. Springer, New York, NY, US.
142. **Danecek P, Auton A, Abecasis G, Albers CA, Banks E, DePristo MA, Handsaker RE, Lunter G, Marth GT, Sherry ST, et al.**. 2011. The variant call format and VCFtools. Bioinformatics 27 (15):2156–2158.
143. **Team RC**. 2016. R Foundation for statistical computing. R: a language environment for statistical computing .
144. **Bates D, Sarkar D, Bates MD, Matrix L**. 2007. The lme4 package. R Package Version 2 (1):74.
145. **Cockerham CC**. 1963. Estimation of genetic variances. Stat Genet Plant Breed 982:53–94.
146. **Muir W, Nyquist W, Xu S**. 1992. Alternative partitioning of the genotype-by-environment interaction. Theor Appl Genet 84 (1-2):193–200.
147. **Batstone RT, Peters MA, Simonsen AK, Stinchcombe JR, Frederickson ME**. 2020. Environmental variation impacts trait expression and selection in the legume–rhizobium symbiosis. Am J Bot 107 (2):195–208.
148. **Searle SR, Speed FM, Milliken GA**. 1980. Population marginal means in the linear model: an alternative to least squares means. The Am Stat 34 (4):216–221.
149. **Burghardt LT, Epstein B, Tiffin P**. 2019. Legacy of prior host and soil selection on rhizobial fitness in planta. Evolution 73 (9):2013–2023.
150. **Zhou X, Stephens M**. 2014. Efficient multivariate linear mixed model algorithms for genome-wide association studies. Nat Methods 11 (4):407–409.
151. **Quinlan AR, Hall IM**. 2010. BEDTools: a flexible suite of utilities for comparing genomic features. Bioinformatics 26 (6):841–842.
152. **Rockman MV**. 2012. The QTN program and the alleles that matter for evolution: all that's gold does not glitter. Evolution 66 (1):1–17.
153. **Korte A, Farlow A**. 2013. The advantages and limitations of trait analysis with GWAS: a review. Plant Methods 9 (1):1–9.
154. **Tibbs Cortes L, Zhang Z, Yu J**. 2021. Status and prospects of genome-wide association studies in plants. The Plant Genome 14 (1):e20077.
155. **Lasky JR, Forester BR, Reimherr M**. 2018. Coherent synthesis of genomic associations with phenotypes and home environments. Mol Ecol Resour 18 (1):91–106.
156. **Lorts CM, Lasky JR**. 2020. Competition× drought interactions change phenotypic plasticity and the direction of selection on Arabidopsis traits. New Phytol 227 (4):1060–1072.
157. **Lau JA, Bowling EJ, Gentry LE, Glasser PA, Monarch EA, Olesen WM, Waxmonsky J, Young RT**. 2012. Direct and interactive effects of light and nutrients on the legume-rhizobia mutualism. Acta Oecologica 39:80–86.
158. **Heath KD, Podowski JC, Heniff S, Klinger CR, Burke PV, Weese DJ, Yang WH, Lau JA**. 2020. Light availability and rhizobium variation interactively mediate the outcomes of legume–rhizobium symbiosis. Am J Bot 107 (2):229–238.
159. **Huang DW, Sherman BT, Tan Q, Kir J, Liu D, Bryant D, Guo Y, Stephens R, Baseler MW, Lane HC, et al.**. 2007. DAVID Bioinformatics Resources: expanded annotation database and novel algorithms to better extract biology from large gene lists. Nucleic Acids Res 35 (suppl_2):W169–W175.
160. **Sherman BT, Lempicki RA, et al.**. 2009. Systematic and integrative analysis of large gene lists using DAVID bioinformatics resources. Nat Protoc 4 (1):44–57.
161. **Karp PD, Billington R, Caspi R, Fulcher CA, Latendresse M, Kothari A, Keseler IM, Krummenacker M, Midford PE, Ong Q, et al.**. 2019. The BioCyc collection of microbial genomes and metabolic pathways. Briefings Bioinform 20 (4):1085–1093.
162. **Caspi R, Billington R, Keseler IM, Kothari A, Krummenacker M, Midford PE, Ong WK, Paley S, Subhraveti P, Karp PD**. 2020. The MetaCyc database of metabolic pathways and enzymes- a 2019 update. Nucleic Acids Res 48 (D1):D445–D453.
163. **Barnett MJ, Long SR**. 2018. Novel genes and regulators that influence production of cell surface exopolysaccharides in Sinorhizobium meliloti. J Bacteriol 200 (3):e00501–17.
164. **Baev N, Schultze M, Barlier I, Ha DC, Virelizier H, Kondorosi E, Kondorosi A**. 1992. *Rhizobium nod*M and *nod*N genes are common nod genes: *nod*M encodes functions for efficiency of nod signal production and bacteroid maturation. J Bacteriol 174 (23):7555–7565.
165. **Marie C, Barny MA, Downie J**. 1992. *Rhizobium leguminosarum* has two glucosamine syntheses, *gim*S and *nod*M, required for nodulation and development of nitrogen-fixing nodules. Mol Microbiol 6 (7):843–851.
166. **Cao Y, Miller SS, Dornbusch MR, Castle SS, Lenz P, Ferguson J, Sadowsky MJ, Nelson MS, Klatt C, Samac DA**. 2018. Widespread occurrence of Sinorhizobium meliloti strains with a type IV secretion system. Symbiosis 75 (2):81–91.
167. **Paço A, da Silva J, Eliziário F, Brígido C, Oliveira S, Alexandre A**. 2019. *tra*G Gene Is Conserved across *Mesorhizobium* spp. Able to Nodulate the Same Host Plant and Expressed in Response to Root Exudates. BioMed Res Int 2019.

bioRχiv Submission Template bioRχiv Submission Template bioRχiv Submission Template bioRχiv Submission Template bioRχiv Submission Template bioRχiv Submission Template bioRχiv Submission Template

SUPPLEMENTAL MATERIALS

Methods
Results
References 139-169
Datasets S1 to S7
Figures S1 to S12

SUPP. METHODS

Study system. *Medicago truncatula* Gaertn. is an annual legume native to the Mediterranean region in Southern Europe and Northern Africa, and it also occurs in Asia. It lives in a symbiotic association with nitrogen-fixing bacteria in the genus *Ensifer* (formerly *Sinorhizobium*) and has been used as a model-organism to study symbiotic interactions. We used two lines of *Medicago truncatula* in this experiment: A17 (Australia) and DZA 315.16 (Algeria; hereafter abbreviated as DZA). These lines and have been leveraged in studies establishing the role of variable plant-encoded nodule-specific cysteine rich peptides (NCRs, specifically those encoded by *nfs*1 and *nfs*2) in governing the level of nitrogen fixed (Fix+, Fix–, or intermediate) in particular host and strain combinations (137, 138, 139, 121); these lines are included in the *Medicago* HapMap panel of re-sequenced GWAS lines and RIL parents (http://www.medicagohapmap.org). We used 191 strains of the rhizobium *E. meliloti* in this study, which were isolated from the nodules of *M. truncatula* plants grown in soils from 24 sites in Corsica, France and Spain, as part of a larger effort to understand coevolution in this legume-rhizobium mutualism (140, 105).

Experimental design. Seeds were scarified with either a razor blade or sandpaper, then sterilized by first rinsing with 95% EtOH followed by soaking in commercial bleach (6% hypochlorite) for 7 min, rinsed thoroughly with water, and imbibed in ddH_2O overnight at 4°C in the dark. Seeds were then transplanted into sterilized 107 ml SC7 Cone-tainers (Stuewe & Sons Inc., Tangent, OR), each containing an autoclave-sterilized mixture of Turface MVP calcined clay (Profile Products LLC, Buffalo Grove, IL) and the UIUC greenhouse's root wash mix (1:1:1 soil–calcined clay–torpedo sand) in equal volumes, for a final mixture of 1:4:1 soil–calcined clay–torpedo sand. Pots were randomized into racks in the greenhouse, with 10 pots per rack, and racks were evenly arranged across three benches.

E. meliloti cultures were grown in liquid tryptone-yeast (TY) medium (141) for 18-20 hrs at 30°C. Before inoculation, the cell density of each culture was measured with NanoDrop 2000c spectrophotometer (Thermo Fisher Scientific) and adjusted to $\sim 10^6$ cells/ml (OD_{600} = 0.1) by diluting the cultures with sterile TY medium, when necessary. Each plant was inoculated with 500 ml of liquid culture 10-12 days after seeds were planted, and the soil surface received a thin (~0.5 cm) layer of sterile sand after inoculation to minimize cross-contamination. Plants were misted (1/2" M NPT upright misting nozzle, Senninger Irrigation Inc., Clermont, FL) four times per day for 45 min at a time for the first two weeks after transplant, and 30 min at a time thereafter. Plants were given supplemental lighting up to to 14 hr day length and were not fertilized throughout the experiments.

Data collection. For each experiment, we measured plant height, leaf number, and chlorophyll content at four weeks after planting. Chlorophyll was measured using a SPAD 502 Plus (Spectrum Technologies, Inc. Aurora, IL); we recorded the mean of

bioRχiv Submission Template bioRχiv Submission Template bioRχiv Submission Template bioRχiv Submission Template bioRχiv Submission Template bioRχiv Submission Template bioRχiv Submission Template

three measurements on the most recently emerged leaf. At the time of harvest, we counted total root nodules and collected 10 nodules from each plant to estimate per-nodule fresh weight. Shoots and roots were dried and weighed to determine the dry biomass of each plant.

Rhizobium genomic data. Full details are available in Riley et al. (105). Briefly, strains were grown as described above. Rhizobium genomic DNA was extracted and sequenced, followed by quality control and variant calling as described in Riley et al. (105). Variant data were hard-filtered using vcftools (v0.1.17, 142) to include variants with quality scores above 20. Multi-nucleotide polymorphisms were retained as single variants and sites that lacked genotype calls for more than 20% of the strains were removed. We included in the analyses only variants that had a minor allele frequency (MAF) of $\leq 5\%$. We found 491,227 variants represented in our genomes. After filtering for quality and frequency, 36,526 variants remained.

Phenotypic analyses. Within the R environment (143), we implemented linear mixed models (LMMs) using the R package lme4 (v1.1-27.1, 144) to test for G $\times$ E between 191 strains of rhizobia (G) and the two greenhouse experiments (E) for each plant line separately. We additionally partitioned G $\times$ E interactions into variance versus crossing effects using Cockerham's method (145, 146, 147). We square root-transformed all phenotypic variables to improve the normality of the data. For all phenotypic traits (shoot biomass, leaf number, plant height, chlorophyll content), the model included experiment and strain, and their interaction as fixed effects. Rack was included as an additional random effect. From these models, we calculated estimate marginal means for each strain using the emmeans package (v1.4.1, 148).

Our experimental design, which featured two experiments nested within each host genotype, allows robust statistical estimation of G × E, but is underpowered to test for G × G interactions for partner quality phenotypes using ANOVA. Nevertheless a separate study (K. Heath, unpublished data) featuring a subset (N = 20) of the strains from the current study provides strong statistical support for G × G interactions for partner quality in this system (e.g., plant x strain G × G; $\chi^2 = 83.3$; $p < 0.0001$ for plant aboveground biomass; **Supp. Fig. S11**), similar to several other studies in this system (e.g., 28, 118, 120, 149, 123). We additionally calculated the broad-sense heritability ($H^2 = \frac{V_G}{V_P}$) for rhizobium strains within each experiment using LMMs in which response variables were square root-transformed, and both strain and rack were included as random effects. The significance of V_G was assessed by comparing the full model to one in which the strain term was excluded, and a log-likelihood ratio test was performed between the two models to assess whether the proportion of variation explained (PVE) by the strain term was significant. Given the complex multivariate nature of our data at both the phenotypic and genomic levels, we focus the main text on shoot biomass, our core metric of partner quality; results for all other traits (i.e., leaf chlorophyll A, plant height, leaf number) can be found in the Supplementary Materials.

Genome-wide association studies. We performed multiple genome-wide association studies (GWAS) to identify rhizobium genomic variants associated with symbiotic partner quality. We conducted association tests for partner quality traits measured on plant hosts using a LMM approach to GWAS as implemented in the program GEMMA (v0.98.1, 150). Mapping analyses were performed separately for each of the four experiments, on standardized emmeans that corrected for the effects of rack (see above). GWAS relies on variants that are statistically distinguishable from one another (i.e., are not closely linked), and so we first identified genetic variants in strong linkage disequilibrium by splitting variants from all three rhizobia genomic elements into link-

bioRχiv Submission Template bioRχiv Submission Template bioRχiv Submission Template bioRχiv Submission Template bioRχiv Submission Template bioRχiv Submission Template bioRχiv Submission Template

age groups based on the LD threshold $r_2 \geq 0.95$ using a customized script available at the Dryad repository associated with Epstein et al. (45) (https://datadryad.org/stash/dataset/doi:10.5061/dryad.tn6652t), and picked a representative variant from each linkage group with the highest minor allele frequency and least missing data when ties were present (45). We ended up with 6,512 unlinked variants, 600 of which were on the chromosome, 1,797 were on pSymA, and 4,115 were on pSymB. We used selected variants to compute standardized kinship (k) matrices in GEMMA using the - gk 2 option, one for each genomic element, and performed the GWAS mapping using the lmm -4 option. In order to ensure our methods of calculating the k-matrix did not influence the results, we also conducted additional association tests for shoot biomass using k-matrices constructed for: 1) the entire genome (all three replicons together), and 2) for all variants, rather than those filtered by LD. However, our results were comparable regardless of the method used for calculating the k-matrix (**Supp. Fig. S12**), and thus, we only present results based on the initial method.

We assigned significance to particular variants using a permutation test which randomizes genotypes with respect to phenotypes, runs the resulting LMM in GEMMA 1000 times, and then tags loci from the non-randomized run that fell above the 95% false discovery rate cut off (45, 66). Based on these significance tests, we first summarized variants to the gene-level, in which we identified the genes closest to or encompassing our significant variants using the intersect option in bedtools (v2.29.2, 151), and excluded any intergenic regions.

Finally, we were interested in the genetic basis of environmental-dependency (i.e., "G × E" genes), where the allelic effects varied among experiments within a particular host genotype due to either conditional neutrality (i.e., significant effects on the phenotype in one environment but not the other) or antagonistic allelic effects (i.e., significant effects in both environments, but in the opposite direction). Because mapping experiments suffer from false negatives (152), the lack of a significant association in one experiment does not rigorously identify patterns of conditional neutrality at the individual locus or at the global (whole genome) level (152, 153, 154). Thus we took multiple approaches to inspecting G × E in our association analyses. First, we used cross-environment correlations between the estimated effects from each experiment (computed independently, see above) to visually assess the degree to which allelic effects were consistent across experiments (within a host genotype) and identify antagonistic allelic effects (loci with significant, but opposite, effects in the two experiments). Next, to test the global null hypothesis that the direction and magnitude of the estimated rhizobium allelic effects were consistent across the two experiments for a particular host (i.e., that allelic effects estimated in the two environments fell along the 1:1 line), we used a permutation test wherein we first resampled the estimated effects from the first experiment (i.e., DZA experiment I) with experimental error (standard deviation) and calculated the slope of their correlation, repeated this for 1000 permutations, then computed the probability of our observed slope given this simulated null distribution. Beyond this global test, to rigorously identify individual loci that contribute to the environmental response, we calculated plasticity for each strain (155, 156); plasticity was calculated as the natural log of the response ratio of the phenotype across experiments (e.g., $log(\frac{\text{shoot biomass exp. 3 (DZA)}}{\text{shoot bioamss exp. 1 (DZA)}})$; Lau et al. 157, Heath et al. 158) and mapped this trait separately for each of the two host genotypes.

Candidate gene functional analyses. To explore the biological interpretation of our various gene lists (e.g., A17-only, Experiment 1, Universal; see results), we used DAVID Bioinformatics Resources (v.6.8, 159) to test for significantly overrepresented UNIPROT keywords, GO terms, and KEGG pathways, as described in Sherman et al.

bioRχiv Submission Template bioRχiv Submission Template bioRχiv Submission Template bioRχiv Submission Template bioRχiv Submission Template bioRχiv Submission Template bioRχiv Submission Template

(160). We report the results of enrichment analyses as "marginal" when the pre-FDR p-value associated with the EASE modified Fisher exact test was < 0.05 and "significant" when FDR-corrected p-value was < 0.05. We explored key pathways and genes implicated in particular gene sets using BioCyc (161, 162).

SUPP. RESULTS

We interrogated the gene sets from two key studies that have associated natural variation in *E. meliloti* genomes with symbiotic partner quality (see **Supp. Dataset S2**, "overlap" column; Epstein et al. 45, Batstone et al. 66). Our nearly-universal gene set contained eight loci that overlapped with the top 100 associations with A17 biomass from Epstein et al. (45). Most notable is the fructose-6-phosphate aminotransferase *nod*M/*glm*S (SMa0878/NP_435728.1) that catalyzes a precursor of both peptidoglycan and Nod factor in the glucosamine biosynthesis pathway. This locus is located in the symbiosis gene region of pSymA, though a paralog exists on the chromosome (SMc00231/NP_385762.1; Barnett and Long 163). Knockout mutants of *nod*M are known to decrease N-fixation of *E. meliloti* on alfalfa (164) and *Rhizobium leguminosarum* (165); together with Epstein et al. (45), our studies highlight the role of natural variation in bacterial glucosamine metabolism in determining plant health. We also found six genes in this nearly-universal set that were also associated with symbiotic partner quality, rhizobium fitness, or both in the experimental evolution study of Batstone et al. (66). Most notable are two *tra* (transfer) loci (*tra*A2 on pSymB and *tra*G on pSymA), potentially part of a Type IV Secretion System (T4SS) responsible for targeting proteins to host cells (166, 167). While the variants we found in these loci are segregating in natural populations in the native range of *E. meliloti*, these loci also evolved *de novo* in response to passaging through the same host for multiple generations (66), making them strong candidates for a consistent role in symbiosis.

SUPP. DATASETS

- Dataset S1: **"SNPs_ann_ps_shoot.wREADME.xlsx"**
  Summary table for all variants significantly associated with shoot biomass in any of the four experiments. The first tab "SNPs_ann_ps_shoot" provides variant-level information, while the "README" tab provides a brief description of each column in the first tab.
- Dataset S2: **"genes_shoot_uniprot.wREADME.xlsx"**
  Summary table for all genes containing variants significantly associated with shoot biomass in any of the four experiments. The first tab "genes_shoot_uniprot" provides gene-level information, while the "README" tab provides a brief description of each column in the first tab.
- Dataset S3: **"SNPs_ann_ps_all.wREADME.xlsx"**
  Summary table for all variants significantly associated with one or more partner quality traits in any of the four experiments. The first tab "SNPs_ann_ps_all" provides variant-level information, while the "README" tab provides a brief description of each column in the first tab.
- Dataset S4: **"SNPs_ann_gene_all.wREADME.xlsx"**
  Summary table for all genes containing variants significantly associated with one or more partner quality traits. The first tab "SNPs_ann_gene_all" provides gene-level information, while the "README" tab provides a brief description of each column in the first tab.

bioRχiv Submission Template bioRχiv Submission Template bioRχiv Submission Template bioRχiv Submission Template bioRχiv Submission Template bioRχiv Submission Template bioRχiv Submission Template

- Dataset S5: **"DAVID_outputs_combined.wREADME.xlsx"**
  Summary table for all genes run through DAVID for which terms (GO, UNIPROT, KEGG pathways, et c.) were significantly (or marginally) enriched. The first tab "DAVID_outputs_combined" provides gene-level information, while the "README" tab provides a brief description of each column in the first tab.
- Dataset S6: **"plast_overlap_shoot.wREADME.xlsx"**
  Summary table for all genes containing variants significantly associated with either shoot biomass or plasticity for shoot biomass or both (i.e., overlapping). The first tab "plast_overlap_shoot" provides gene-level information, while the "README" tab provides a brief description of each column in the first tab.
- Dataset S7: **"genes_shoot.plast.wREADME.xlsx"**
  Summary table for all genes containing variants significantly associated with plasticity based on shoot biomass. The first tab "genes_shoot.plast" provides gene-level information, while the "README" tab provides a brief description of each column in the first tab.

bioRχiv Submission Template bioRχiv Submission Template bioRχiv Submission Template bioRχiv Submission Template bioRχiv Submission Template bioRχiv Submission Template bioRχiv Submission Template bioRχiv Submission Template

SUPP. FIGURES

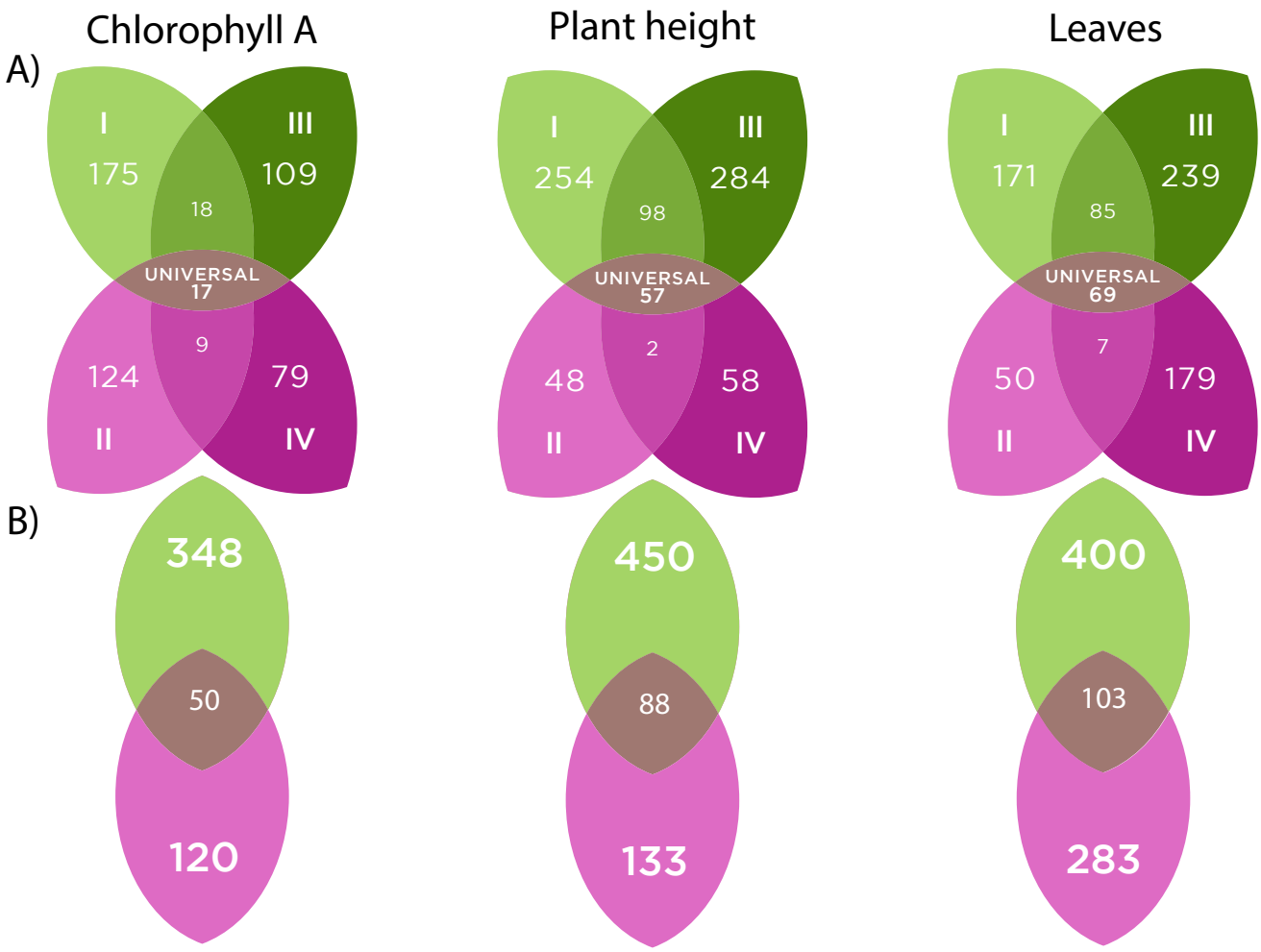

Supp. Figure S1 **Genes underlying G × E are prevalent across partner quality traits. Venn diagrams showing number of rhizobium (*E. meliloti*) genes significantly associated with three other partner quality phenotypes for A) each of four separate mapping experiments or B) cross-experiment plasticity for either host genotype DZA in green (experiments I and III, in green) or A17 (experiments II and IV in pink). The mauve oval in the center represents either A) universal genes that contribute to trait variation in at least three of the four experiments or B) genes associated with cross-experiment trait plasticity in both host genotypes.**

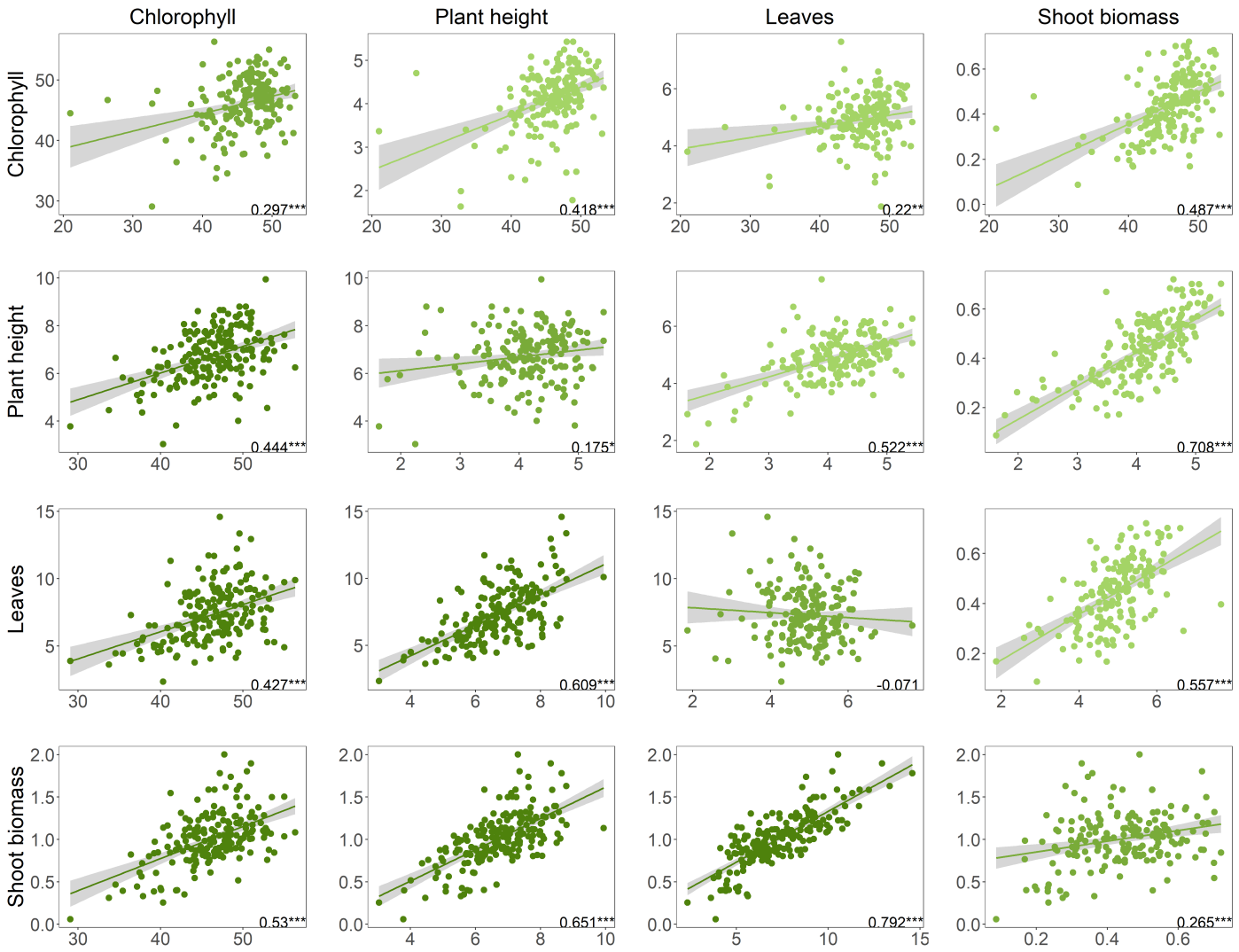

Supp. Figure S2 **Genetic correlations for traits measured on DZA. Genetic correlations among traits within experiments (above or below diagonal) or between the same trait across experiments (along diagonal). Correlations based on estimated marginal means of each rhizobia strain corrected for rack on plant line DZA. Numbers in bottom right corners of each plot indicate Pearson correlation coefficients. Plots above and below the diagonal are for traits measured in experiments 1 and 3, respectively. Significance: $p < 0.001$ = '***'; $p < 0.01$ = '**'; $p < 0.05$ = '*'.**

bioRχiv Submission Template bioRχiv Submission Template bioRχiv Submission Template bioRχiv Submission Template bioRχiv Submission Template bioRχiv Submission Template bioRχiv Submission Template

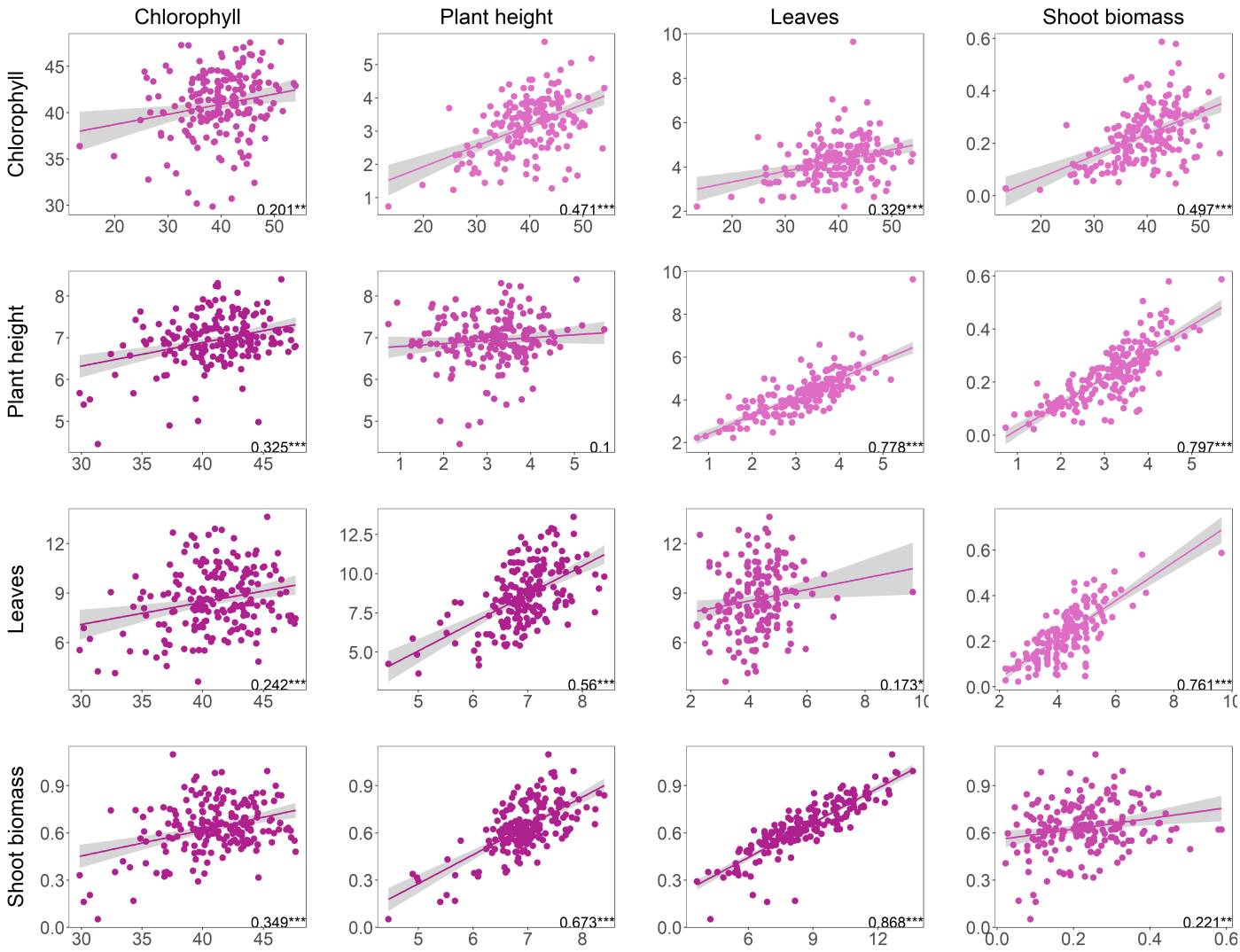

Supp. Figure S3 **Genetic correlations for traits measured on A17. Genetic correlations among traits within experiments (above or below diagonal) or between the same trait across experiments (along diagonal). Correlations based on estimated marginal means of each rhizobia strain corrected for rack on plant line A17. Numbers in bottom right corners of each plot indicate Pearson correlation coefficients. Plots above and below the diagonal are for traits measured in experiments 2 and 4, respectively. Significance: $p < 0.001$ = '***'; $p < 0.01$ = '**'; $p < 0.05$ = '*'.**

bioRχiv Submission Template bioRχiv Submission Template bioRχiv Submission Template bioRχiv Submission Template bioRχiv Submission Template bioRχiv Submission Template bioRχiv Submission Template

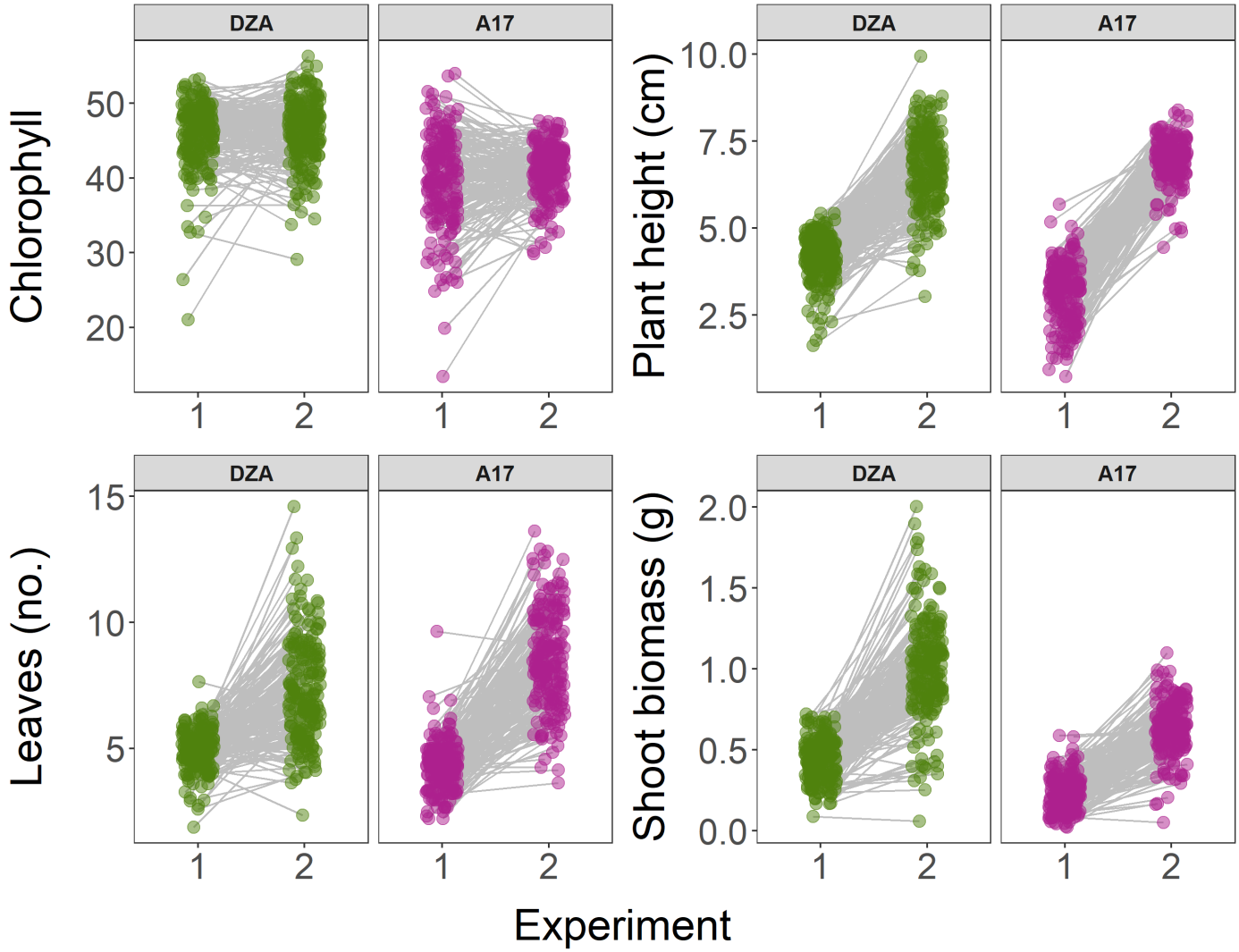

Supp. Figure S4 **Extensive G × E between experiments. Reaction norms for partner quality traits across experiments. Data points represent estimated marginal means corrected for rack within each experiment. Points in green for means estimated on DZA, purple for A17.**

bioRχiv Submission Template bioRχiv Submission Template bioRχiv Submission Template bioRχiv Submission Template bioRχiv Submission Template bioRχiv Submission Template bioRχiv Submission Template

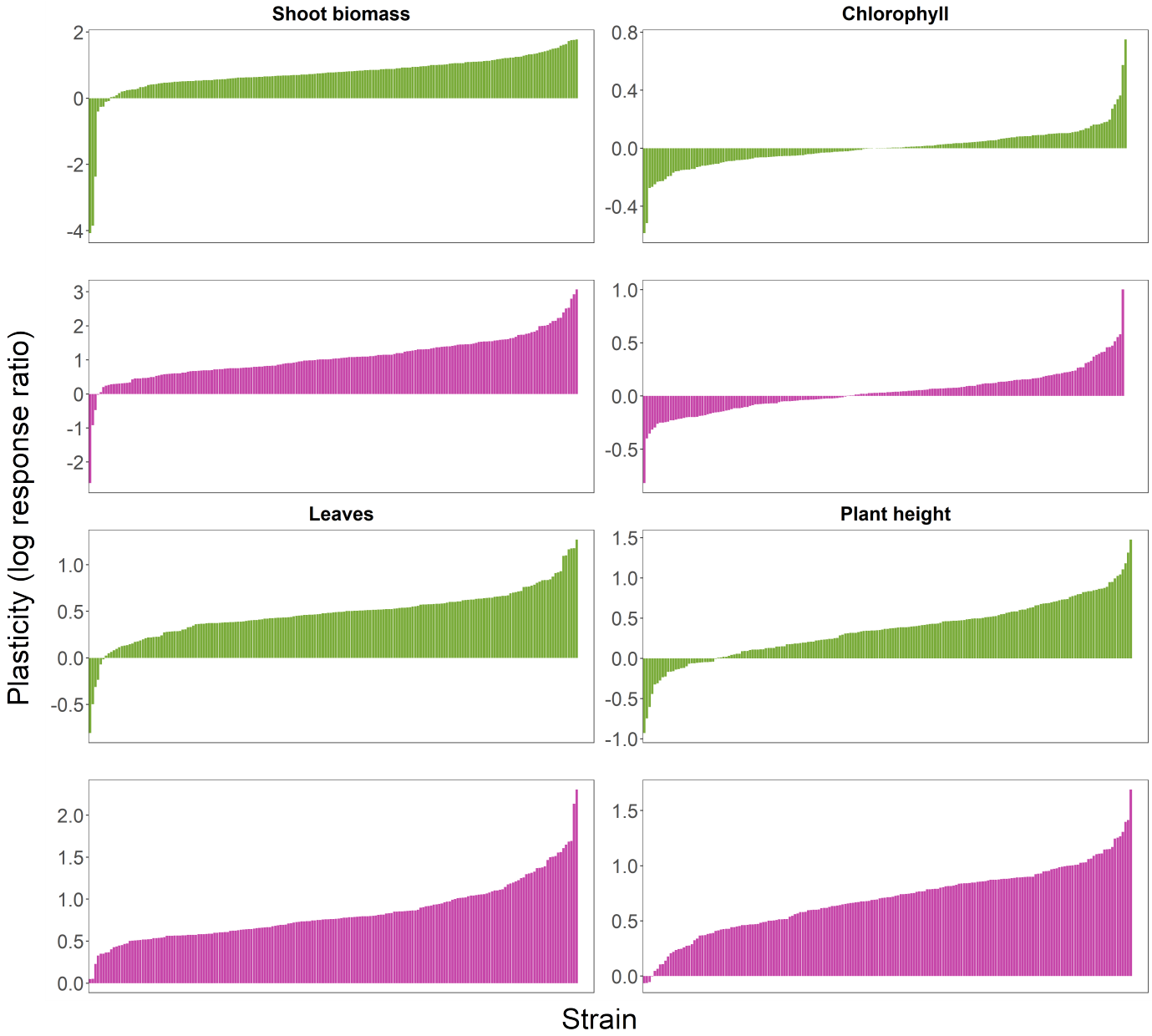

Supp. Figure S5 **Strains significantly varied in their response to different experiments. Variation among *E. meliloti* strains in plasticity, calculated as the log response ratio for each trait between the two experiments with each host genotype (experiments 1 & 3 with DZA in green; experiments 2 & 4 with A17 in pink).**

bioRχiv Submission Template bioRχiv Submission Template bioRχiv Submission Template bioRχiv Submission Template bioRχiv Submission Template bioRχiv Submission Template bioRχiv Submission Template

bioRχiv Submission Template bioRχiv Submission Template bioRχiv Submission Template bioRχiv Submission Template bioRχiv Submission Template bioRχiv Submission Template bioRχiv Submission Template

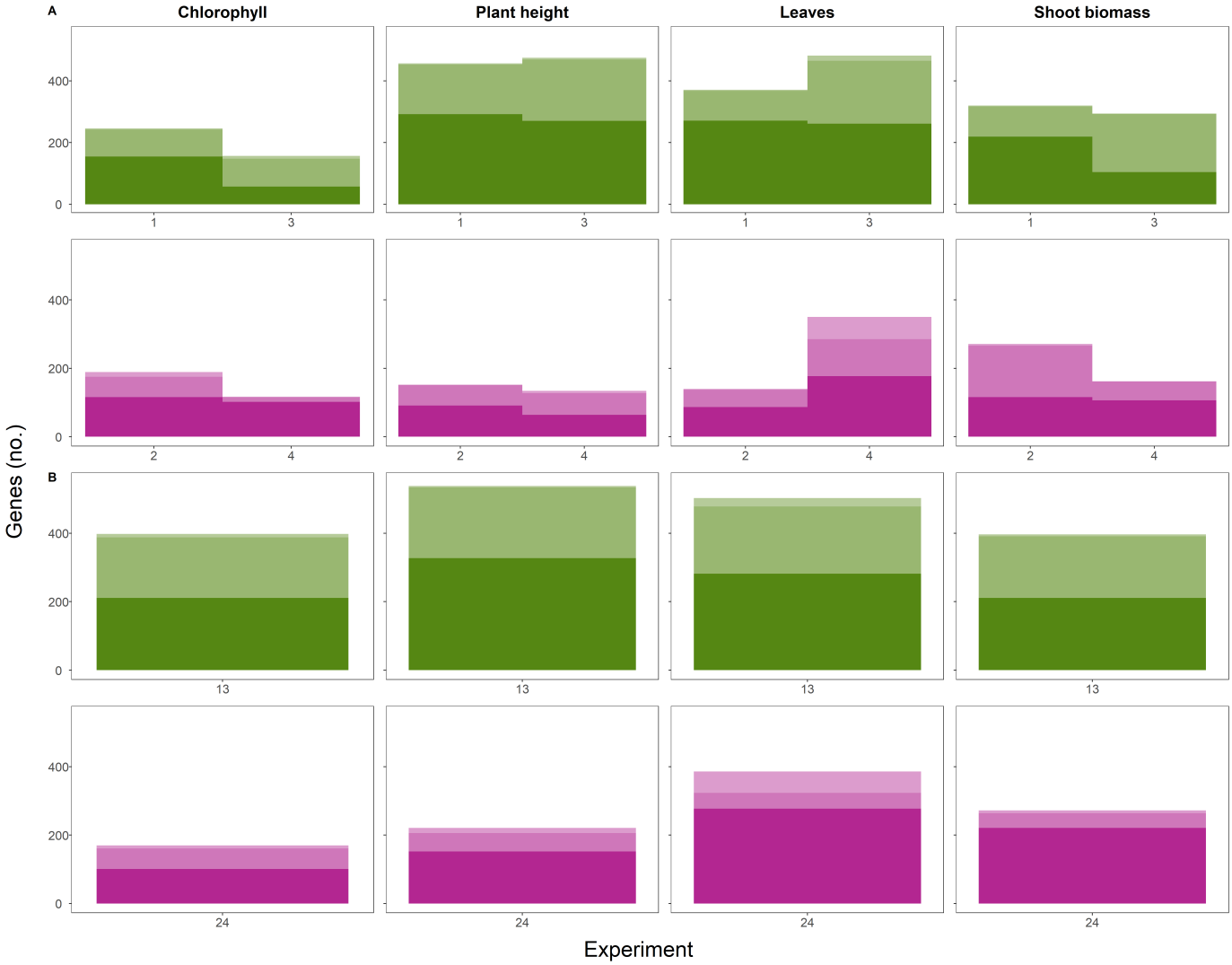

Supp. Figure S6 **Small-scale shifts of loci across genomic regions that contribute to partner quality variation. Distribution of genomic locations (chromosome in lightest shade, pSymA in medium shade, and pSymB in darkest shade) for the *E. meliloti* loci significantly associated with partner quality phenotypes in each of four mapping experiments with either host genotype DZA (green) or host genotype A17 (pink). The plasticity panels (B) represent the genomic locations of rhizobium loci associated with the response of each trait across the two experiments for each host line (1-3 for DZA and 2-4 for A17).**

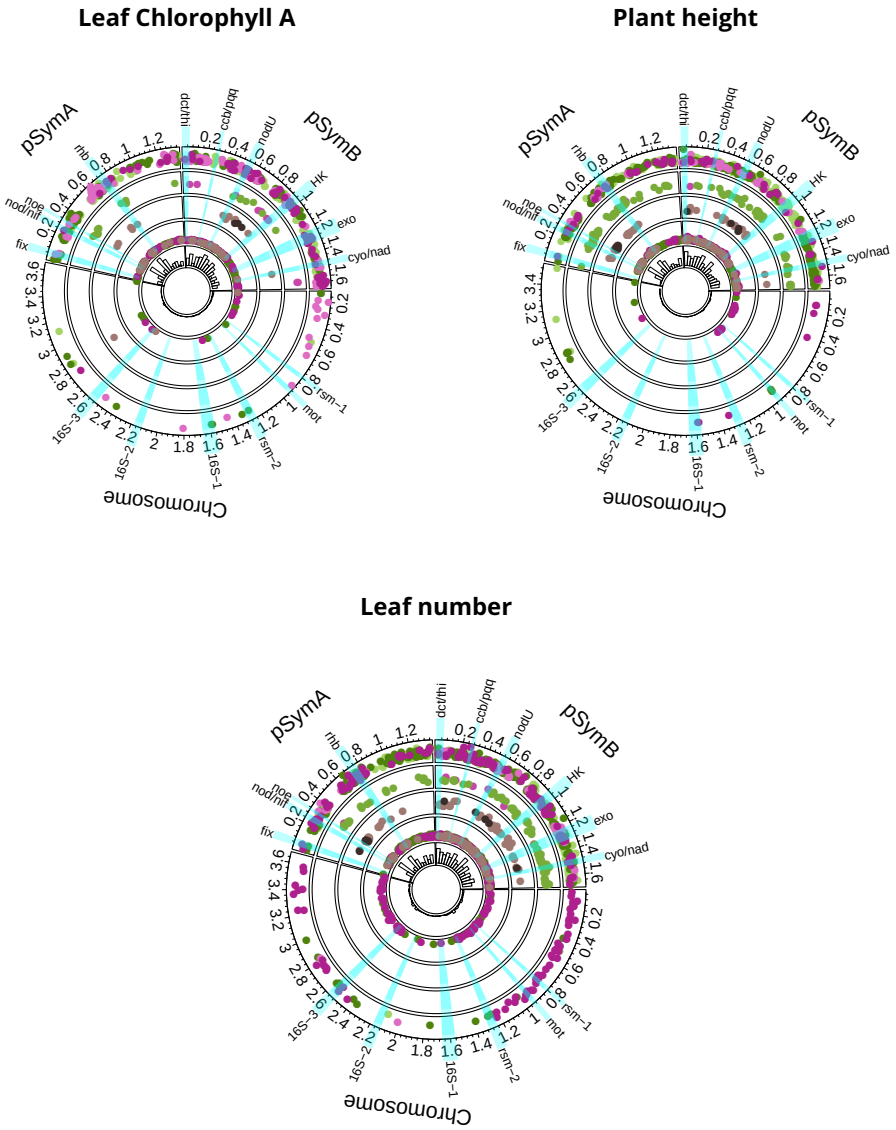

Supp. Figure S7 Loci associated with partner quality are mostly limited to the symbiosis plasmids. Circos plots showing positions of genes (dots) significantly associated with three additional partner quality traits. Each ring represents a different gene category, outermost to innermost: 1) G x E, 2) G x G, 3) partially universal and universal, 4) plasticity, while 5) depicts a histogram based on the total number of significant genes across 100 kbp-sized windows. The x- and y-axes for rings 1-4 represent genomic position (Mbp) and average absolute effect sizes of variants within each gene, respectively. The colours reflect categories in the Venn Diagrams: for rings 1, 2, and 4, genes associated with DZA-only traits are represented by shades of green, on A17-only with shades of purple, and both hosts in mauve (ring 4). For ring 3, genes associated with both hosts in more than three environments are represented in mauve (i.e., "partially universal"), and universal genes in black. Relevant loci are highlighted in blue, with abbreviations for clusters on the outer circle as follows: rsm-1: rsmD,E; ribF; groL; hisG,Z. mot: fliF,I,N,P,Q,R; flgB,D,F,G; motA,B; flhB. rsm-2: sppA; lptB; rpoN; raiA; ptsN; hrcA; rph; rdgB; ubiB; coaBC; iolB-E; cysK; rmsI; pyrF; queG, corA. 16S-1: metB; rrf (5S rRNA); 16S rRNA; hrpB; hisA,H; addA,B; trxA; trpB; hpcH; gyrB; rho. 16S-2: 16S rRNA; rrf (5S rRNA); oppD; glnQ; hppD; hmgA; maiA; purU; lpdA; modC; cobG,H,M. 16S-3: grxC; ptsP; prmC; clpB; 16S rRNA; rrf (5S rRNA); tkt; deoC. fix: nnrU; norD,E; hemN; nirK; napA,E,F; fixG-L,P,Q,S; ccoN-Q; ric; nosR. nod/nif: nolF,G; nodA-C,D,D3,E,F,H,I,J,N; nifA,B,D,E,H,K,N,T,X; fabG; syrA; fdxB; fixA-C. noe: noeA,B; nodL; ccoN2,O2,P2,Q2; nodD2; groL. rhb: selB; fdhE; fdxH; fdnG; repA,B; katG; rhbC,D,F; basC; kdpB,F. dct/thi: urtA-C; dctD; thiC,O,S; mtnA; nspC; paaB,J,I,X. ccb/pqq: fghA; moxF; gfa; cbbX; rbcL; fba; tkt; pqqA,D,E. nodU: ugpC; ehuA-D; eutA,B; doeA,B; uxuA; galE; nodU. HK (housekeeping): alc; uraH; xdhA-C; guaD; pbpC; doeC; hutG,H; ltrA; phnC-E,N; gabD,T. exo: exsH; cueC-E; galE; exoA,F,H,I,K,L,M,O,P,Q,U,V,W,Y; thiD; nirD; nfeD, der; nnrU; bacA; map; glpK; xdhA; guaD; lldD. cyo/nad: cyoA-D; rfaL; minC,D; nadE; asnB.

bioRχiv Submission Template bioRχiv Submission Template bioRχiv Submission Template bioRχiv Submission Template bioRχiv Submission Template bioRχiv Submission Template bioRχiv Submission Template

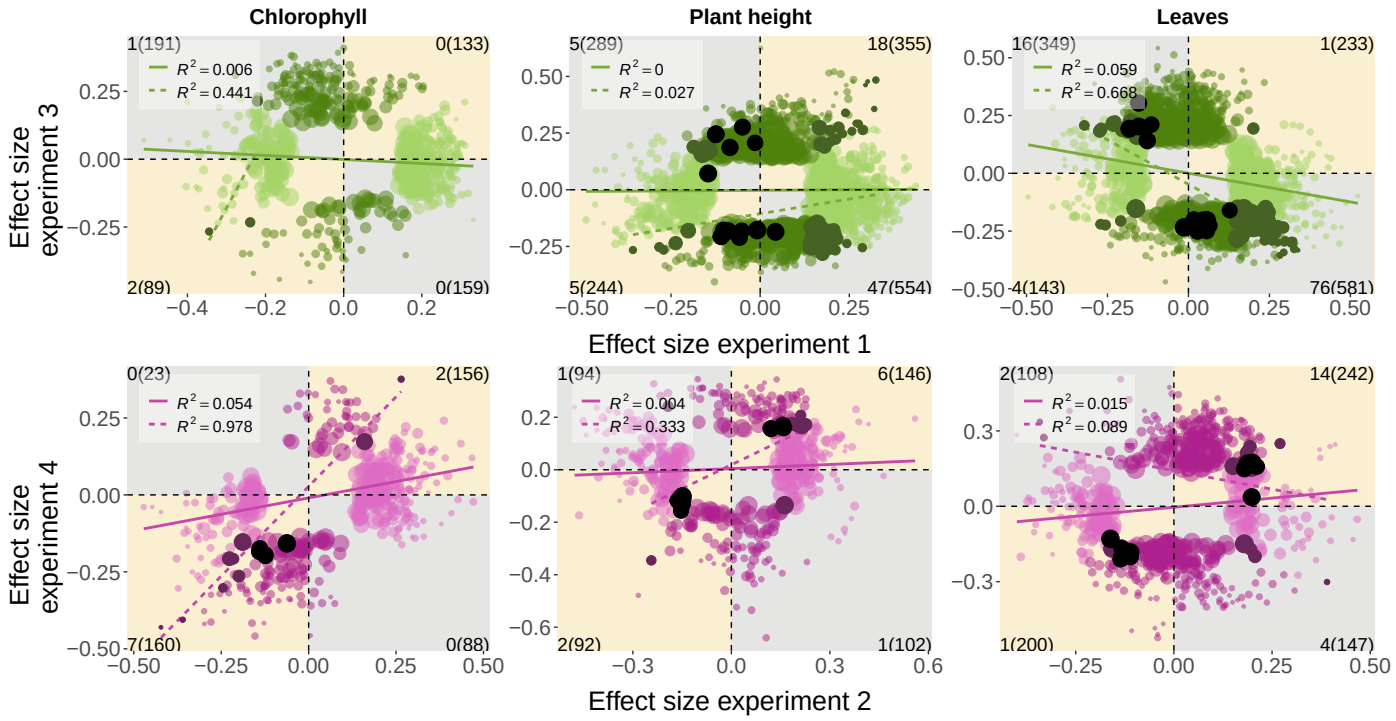

Supp. Figure S8 **Extensive G × E revealed at the variant-level. Variant-level G × E for partner quality loci. Shown are correlations between the estimated effects of individual *E. meliloti* loci on three difference partner quality metrics (from GWAS) in each of two experiments for either host DZA (green) and A17 (pink). Only allelic effects that were significant in one (lighter colours) or both (dark points) environments are shown, while black dots represent nearly universal variants, i.e., associated with the same trait in three experiments. Linear relationships and R^2 values are depicted for all significant variants (solid coloured line) or variants significant in both experiments (dotted coloured line). Variant counts for each quadrant are shown in the corners of each plot (variants significant in both experiments, followed by all variants in parentheses).**

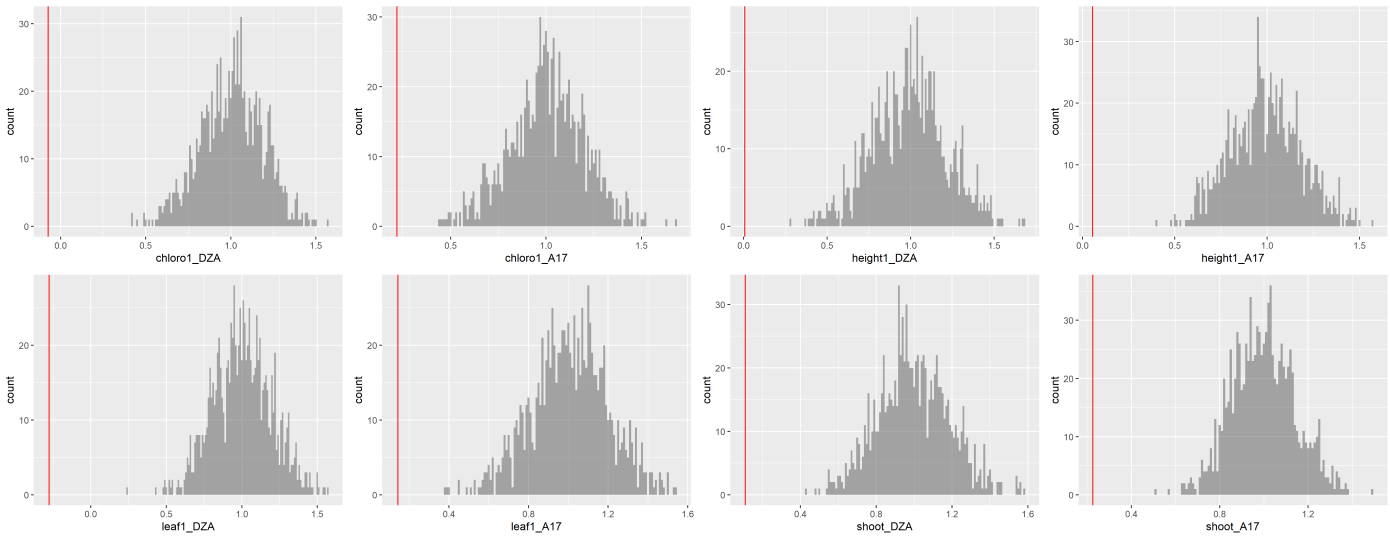

Supp. Figure S9 **Global analyses show that allelic effects are significantly different across experiments. Distributions of slopes calculated by resampling the estimated effects from one experiment (e.g., DZA experiment I) with experimental error (standard deviation), regressing against the observed effects in that experiment, and repeating 1000 times. Red lines depict observed slopes when estimated effects were regressed between experiments.**

bioRχiv Submission Template bioRχiv Submission Template bioRχiv Submission Template bioRχiv Submission Template bioRχiv Submission Template bioRχiv Submission Template bioRχiv Submission Template

bioRχiv Submission Template bioRχiv Submission Template bioRχiv Submission Template bioRχiv Submission Template bioRχiv Submission Template bioRχiv Submission Template bioRχiv Submission Template

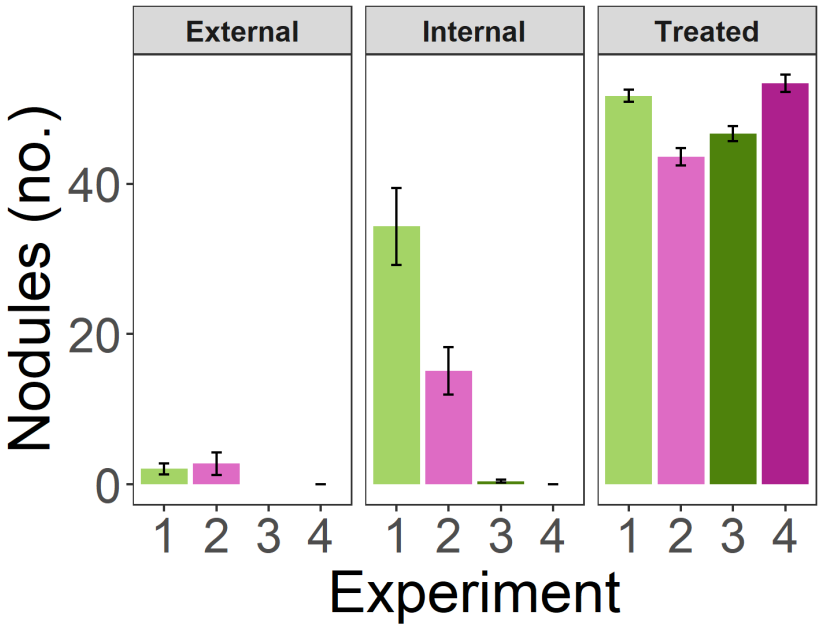

Supp. Figure S10 **Contamination was minimal across experiments. Nodule number for inoculated (i.e., Treated) versus Internal and External uninoculated control plants in four experiments: Experiments 1 and 3 used host genotype DZA (shades of green) while 2 and 4 used genotype A17 (shades of pink).**

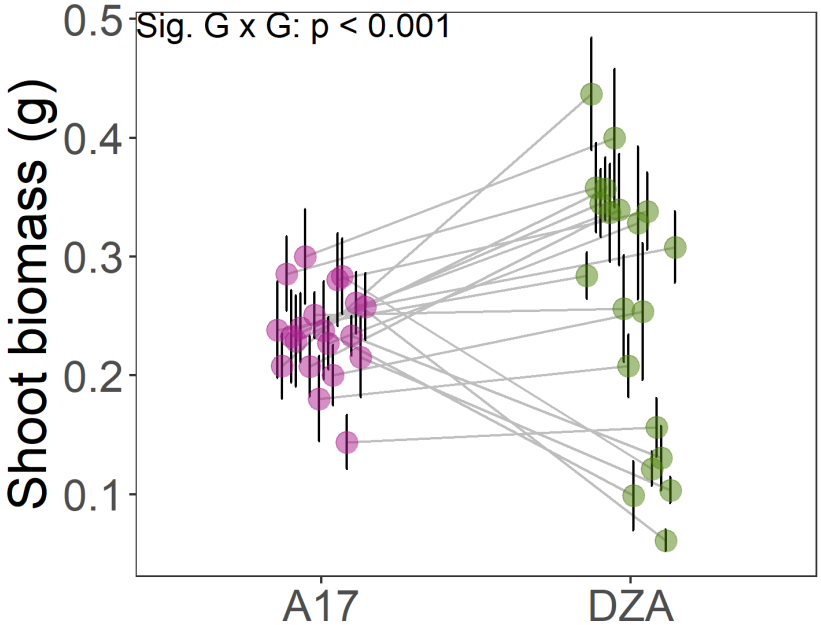

Supp. Figure S11 **Significant Genotype-by-genotype (G × G) interactions between two host genotypes (A17 and DZA) and 20 *E. meliloti* strains. All 20 strains were included in the 191 strains used in current paper. Both hosts were grown together in a single experiment (Heath et al., unpublished data). Type III ANOVA based on a linear mixed model that corrected for rack and researcher was used to test for the main effects of rhizobium strain (χ^2 = 94.891, p < 0.001), host genotype (χ^2 = 0.553, p = 0.457), and strain-by-host (G x G) interaction (χ^2 = 83.272, p < 0.001) on plant shoot biomass.**

bioRχiv Submission Template bioRχiv Submission Template bioRχiv Submission Template bioRχiv Submission Template bioRχiv Submission Template bioRχiv Submission Template bioRχiv Submission Template

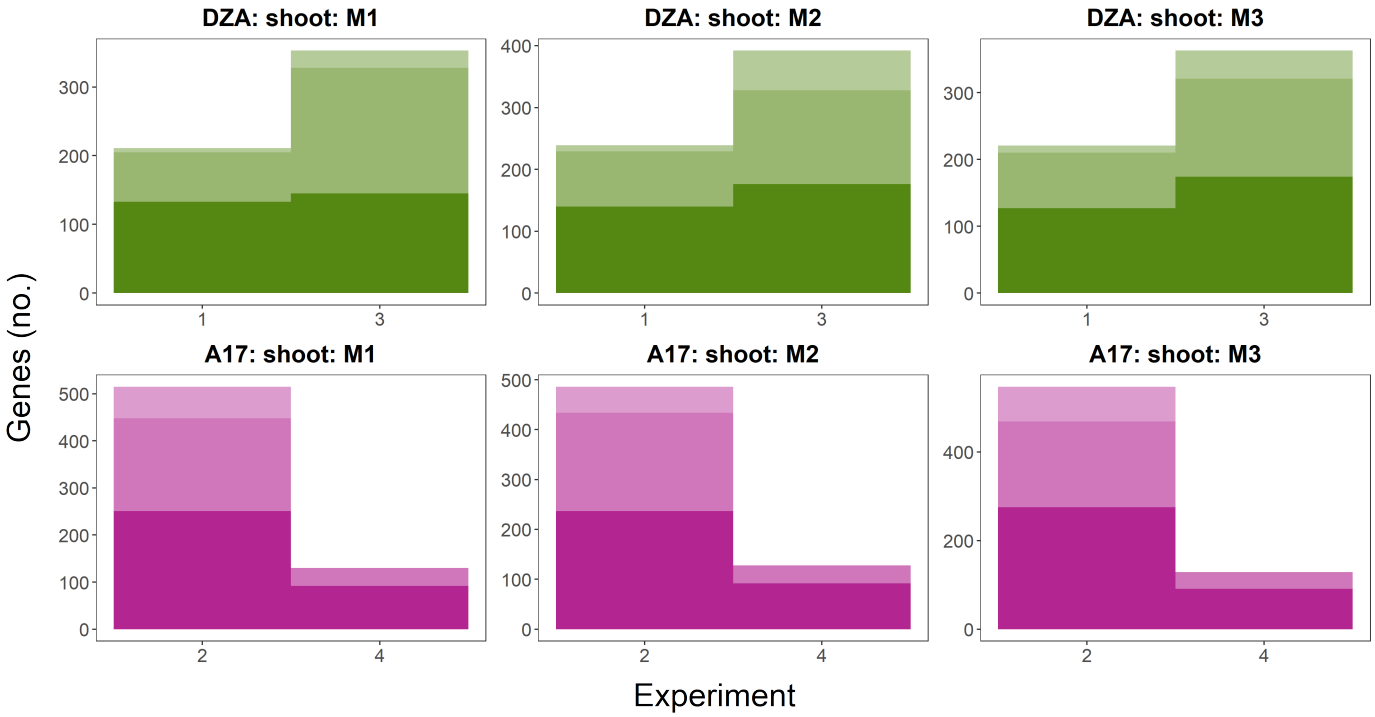

Supp. Figure S12 **Minimal differences in the number of significant genes across three different methods. To ensure the significant variants identified in our study did not depend on the computational methods used (i.e., how the k-matrix was computed), we compared the number of genes tagged by variants significantly associated with shoot biomass in all four experiments and both plant lines (top row in shades of green = DZA; bottom row in shades of pink = A17) for three separate methods: M1) k-matrix calculated for each genomic region separately, only unlinked variants included as input; M2) k-matrix calculated for the whole genome, only unlinked variants included as input; and M3) k-matrix calculated for the whole genome, linked variants included as input. The different shades represent whether genes were located on the chromosome (lightest), pSymA (medium), and pSymB (darkest).**